Rooftop Solar Technical Potential for Low-to-Moderate Income Households in the United States

Benjamin Sigrin and Meghan Mooney
National Renewable Energy Laboratory

Rooftop Solar Technical Potential for Low-to-Moderate Income Households in the United States

Benjamin Sigrin and Meghan Mooney
National Renewable Energy Laboratory

NOTICE

This report was prepared as an account of work sponsored by an agency of the United States government. Neither the United States government nor any agency thereof, nor any of their employees, makes any warranty, express or implied, or assumes any legal liability or responsibility for the accuracy, completeness, or usefulness of any information, apparatus, product, or process disclosed, or represents that its use would not infringe privately owned rights. Reference herein to any specific commercial product, process, or service by trade name, trademark, manufacturer, or otherwise does not necessarily constitute or imply its endorsement, recommendation, or favoring by the United States government or any agency thereof. The views and opinions of authors expressed herein do not necessarily state or reflect those of the United States government or any agency thereof.

This report is available at no cost from the National Renewable Energy Laboratory (NREL) at www.nrel.gov/publications.

Available electronically at SciTech Connect http:/www.osti.gov/scitech

Available for a processing fee to U.S. Department of Energy and its contractors, in paper, from:

> U.S. Department of Energy
> Office of Scientific and Technical Information
> P.O. Box 62
> Oak Ridge, TN 37831-0062
> OSTI http://www.osti.gov
> Phone: 865.576.8401
> Fax: 865.576.5728
> Email: reports@osti.gov

Available for sale to the public, in paper, from:

> U.S. Department of Commerce
> National Technical Information Service
> 5301 Shawnee Road
> Alexandria, VA 22312
> NTIS http://www.ntis.gov
> Phone: 800.553.6847 or 703.605.6000
> Fax: 703.605.6900
> Email: orders@ntis.gov

Cover Photos by Dennis Schroeder: (left to right) NREL 26173, NREL 18302, NREL 19758, NREL 29642, NREL 19795.

NREL prints on paper that contains recycled content.

Acknowledgements

1

Acronyms

ACS	U.S. Census Bureau American Community Survey
ANOVA	Analysis of variance
AMI	area median income
CARE	California Alternate Rates for Energy
CBECS	Commercial Buildings Energy Consumption Survey
CDBG	Community Development Block Grant
CPUC	California Public Utility Commission
DHS	U.S. Department of Homeland Security
DOE / U.S. DOE	U.S. Department of Energy
EERE	U.S. Department of Energy, Office of Energy Efficiency and Renewable Energy
EIA	Energy Information Administration
FEMA	Federal Emergency Management Agency
FMR	fair market rent
FPL	federal poverty level
GWh	gigawatt-hour
GIS	geographic information system
HHS	U.S. Department of Health and Human Services
HSIP	Homeland Security Infrastructure Program
HUD	U.S. Department of Housing and Urban Development
KDE	Kernel Density Estimation
kWh	kilowatt-hour
LEAD	Low-Income Energy Affordability Data
LiDAR	light detection and ranging
LIHEAP	Low Income Home Energy Assistance Program
LMI	low-to-moderate income
MFOO	multi-family owner-occupied building
MFRO	multi-family renter-occupied building
NCES	National Center for Education Statistics
NHGIS	National Historic Geographic Information System
NHPD	National Housing Preservation Database
NLCD	National Land Cover Database
NREL	National Renewable Energy Laboratory
NSRDB	National Solar Radiation Database
OSM	OpenStreetMap
PUMS	public use microdata sample
PV	photovoltaic
RECS	Residential Energy Consumption Survey
ReEDS	Regional Energy Deployment System
REPLICA	Rooftop Energy Potential of Low Income Communities in America
reV	Renewable Energy Potential Model
SFOO	single-family owner-occupied building
SFRO	single-family renter-occupied building
TMY	typical meteorological year

TMY3	Typical Meteorological Year Version 3
TWh	terawatt hour

Executive Summary

Adoption of rooftop solar in the United States primarily has been concentrated in higher-income households (Moezzi et al. 2017; Vaishnav et al. 2017). As technology costs decline and markets expand, however, focus is shifting to increasing solar access in underserved market segments—particularly to low-to-moderate income (LMI) households, or those earning 80% or less of the area median income (AMI). A key policy goal is to expand solar access more equitably to ensure the benefits of solar, including reduced energy burden, increased resilience, and hedge against electricity rate changes are available to all ratepayers. To achieve this goal, a deeper understanding of the potential LMI market is needed. Although LMI households represent about 43% of the U.S. population, it is unknown what proportion live in buildings suitable for PV, how this potential is distributed among the buildings they live in, or what fraction of their electricity needs could be met with rooftop solar.

This report serves to expand upon previous NREL research investigating the technical potential of rooftop solar in the United States, aiming to improve the understanding in the residential sector, particularly for low-to-moderate income households. Technical potential is a metric that quantifies the maximum generation available from a technology for a given region and does not consider the economic or market viability. A unique contribution of this work is to estimate rooftop solar technical potential of residential buildings per U.S. Census Tract by income, building type, and tenure. The underlying data—as documented in Gagnon et al. 2016—are a series of light detection and ranging (LiDAR)–based scans of the building stock in 128 metro regions. Using LiDAR scans, as opposed to aerial imagery, allows researchers to infer the building footprint and the unshaded roof area, azimuth, and tilt for each distinct roof plane, although roof age or other structural concerns are not considered. This data then is intersected with U.S. Census Bureau socio-demographic and building stock data at the tract-level to better understand how rooftop solar technical potential is allocated among different building types. This research also uses statistical techniques to estimate rooftop potential in areas not covered by the LiDAR scans. Collectively, these data and methods are used to address three research questions.

1. **What is the quantity and spatial distribution of rooftop technical potential, stratified by income, building type, and tenure?** At a gross level, these data enable improved estimates of the possible opportunity for deployment, as well as the magnitude of various policy interventions.

2. **Among low-to-moderate-income households, what is the feasibility of achieving parity in solar access across income groups?** Compared to high-income households, LMI households disproportionately live in rental-occupied, multi-family buildings. Because of principal-agent issues in solar adoption, there are significant economic and regulatory barriers inhibiting the installation of solar equipment on buildings occupied by LMI households. This study investigates the feasibility of offsetting at least 33% of LMI household electrical consumption with solar energy and, where infeasible, highlight consideration of novel deployment models—such as community solar, virtual net metering, and other shared solar models.

3. Finally, low- and moderate-income households interact with a vast web of nonprofit entities (e.g., places of worship and public schools). **What is the quantity of technical**

4

potential for these classes of buildings, and to what extent might these buildings "oversize" systems on their roofs to export excess generation to LMI households? Increasing access to solar for such third-parties could reduce these entities' operational costs and indirectly provide roof space to households without access.

National Residential Rooftop PV Technical Potential

Over all tracts and all residential buildings in the United States, the estimated residential rooftop solar technical potential is nearly 1,000 terawatt-hour (TWh) of generation, or about 75% of residential consumption. Significant potential is found in every income group (Table ES-1), with the greatest overall potential in the non-LMI (>80% AMI) income group, and with 416 TWh for low-to-moderate (0% to 80% AMI) households over 25.5 million solar-suitable buildings. The LMI potential is approximately 42% of the total U.S. residential potential, a considerable portion of the overall rooftop opportunity (Figure ES-1).

Table ES-1. National Residential PV Rooftop Technical Potential by Income Group

Income Group		Households (millions)	Suitable Buildings (millions)	Suitable Module Area (millions of m^2)	Capacity Potential (GW$_{DC}$)	Annual Generation Potential (TWh/year)
LMI	Very Low (0%–30% AMI)	19.5	9.4	794.4	127.1	160.8
	Low (30%–50% AMI)	11.5	5.7	472.8	75.6	95.3
	Moderate (50%–80% AMI)	18.8	10.4	792.0	126.7	159.8
Non-LMI	Middle (80%–120% AMI)	21.1	12.3	900.4	144.1	180.8
	High (> 120% AMI)	46.0	29.4	2,003.3	320.5	403.1
All LMI Buildings		49.8	25.5	2,059.2	329.4	415.9
All Residential Buildings		116.9	67.2	4,962.9	794.0	999.8

A majority of the overall residential potential (683 TWh, 68.4%) is situated on single-family buildings, as compared to multi-family dwellings (316 TWh, 31.6%) and single-family potential exceeded multi-family potential for each income group. Similar ratios are seen for owner-occupied and renter-occupied buildings as there is a strong correlation between multi-family occupancy and rental status. For LMI households specifically, the largest modality of potential is for single-family owner-occupied buildings (176.8 TWh), followed by multi-family renter-occupied buildings (140.1 TWh). Though deployment of rooftop solar historically has been concentrated on single-family owner-occupied buildings, nearly 60% of potential for LMI buildings exists on renter-occupied and multi-family buildings.
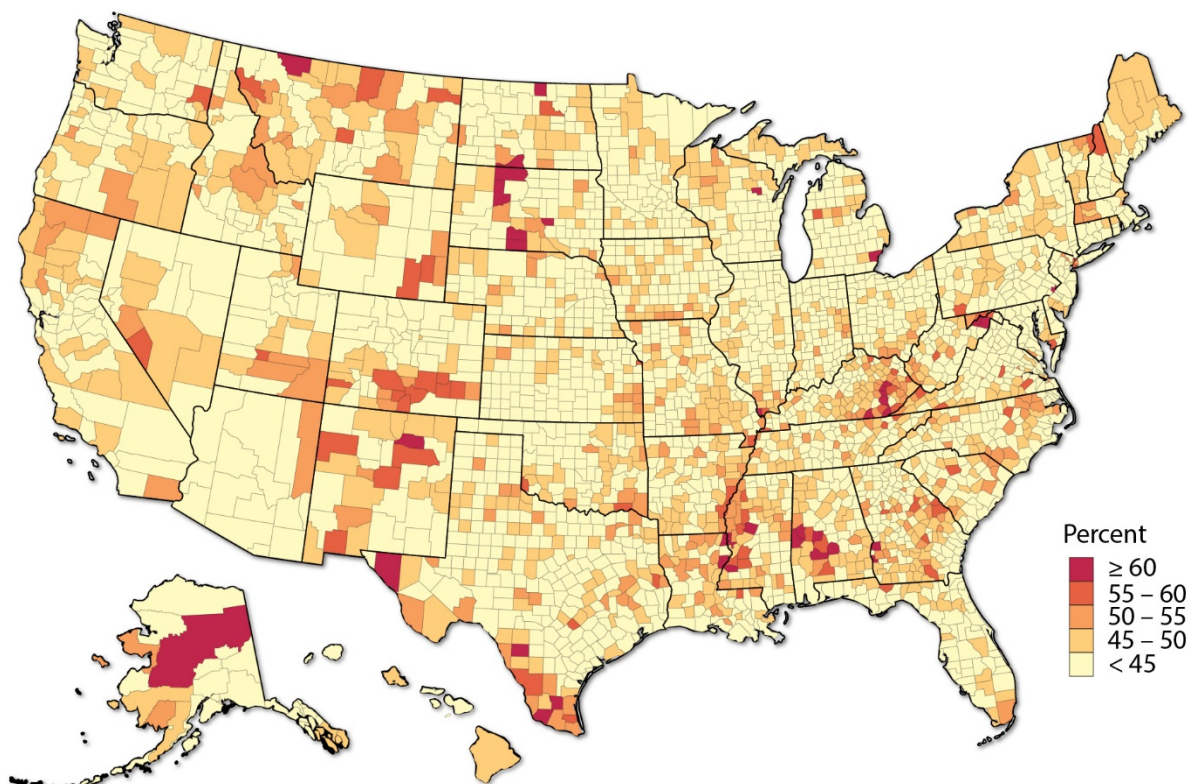
Figure ES-1. County LMI rooftop technical potential as percent of total residential potential

Feasibility of Parity in Adoption Rates

The U.S. Department of Energy (DOE) Solar Energy Technology Office recently announced updated cost targets for solar energy, which could result in 971 GW of solar capacity, providing 33% of electrical generation by 2050 (Cole et al. 2017). Inspired by this goal we investigate the feasibility of rooftop solar offsetting at least 33% of low- and moderate-income household electrical consumption in each U.S. county. Note that the data does not enable assessment of the feasible offset fraction *at the household level*, and instead should be interpreted in aggregate over the county. The analysis also only considers consumption offsets over an annual basis and does not consider hourly mismatches in generation and consumption—which could be substantial without energy storage or other load-shifting methods.

Offsetting 33% of LMI household electrical consumption ("offset target") with rooftop solar is technically feasible on a national scale when only considering households in single-family owner-occupied (SFOO) buildings, although to do so requires buildout on essentially all SFOO buildings—an impractical and unforgiving market challenge. In contrast, on a technical basis, there is more than sufficient roof space to meet the 33% offset target when including single-family rental-occupied (SFRO), multi-family owner-occupied (MFOO), and multi-family renter-occupied (MFRO) buildings (Figure ES-2). Specifically, the average fraction of generation potential to consumption nationally is 85% for the Very Low, 92% for Low, 80% for Moderate, and 70% for Non-LMI income groups. The lower per-capita levels of consumption for low-income households makes offset targets more feasible for this group than for non-LMI households.
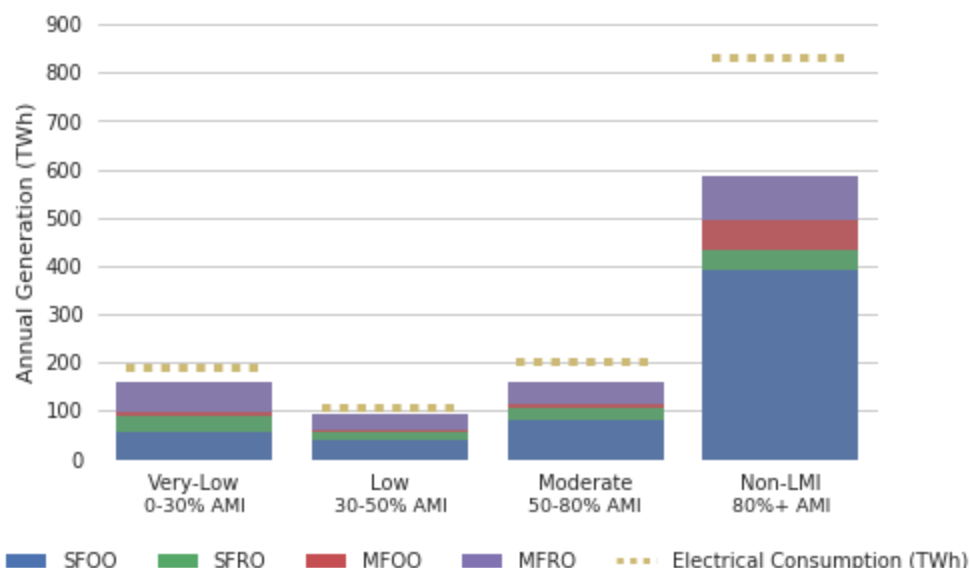
6

Figure ES-2. Technical feasibility of matching residential electrical consumption with rooftop solar (shown by income group)

Not all counties can offset 33% of their LMI consumption with in-county rooftop solar. When considering only single-family owner-occupied buildings, 40% of U.S. counties have insufficient rooftop solar potential to offset 33% of LMI electrical consumption (Figure ES-3 left), though when including the remaining residential building stock this figure decreases to 1% (Figure ES-3 right). In the latter condition, shortfalls are most significant for mobile homes (38 TWh)—whose roofs are typically not suitable for solar, followed by single-family (6 TWh) and multi-family (2 TWh) buildings. Spatial trends in the potential for solar to offset LMI consumption most-strongly reflected regional variation in per-capita electricity consumed, primarily due to which fuels are used for building heating and cooling loads. Other trends include solar irradiance, building-stock composition, and the prevalence of solar-suitable rooftops.
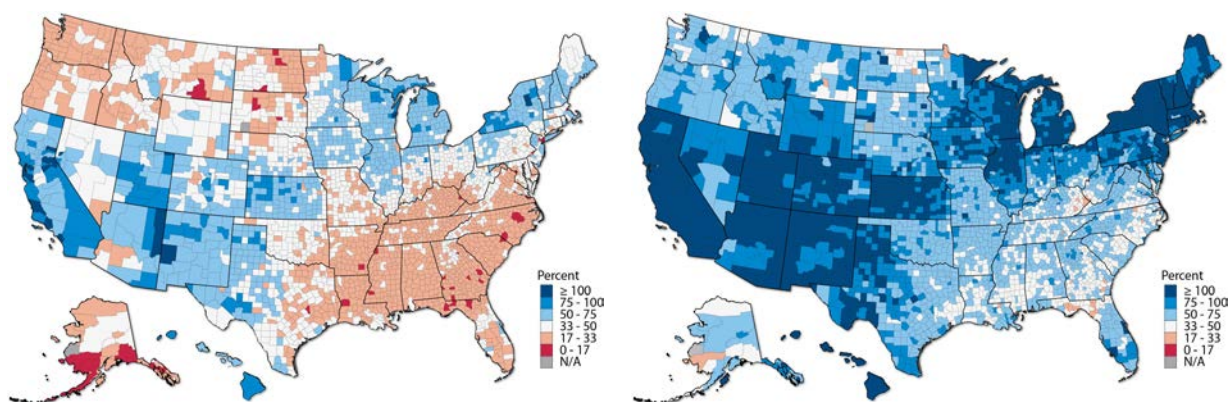

Figure ES-3. Percent of LMI electrical consumption that can be offset by rooftop solar generation—single-family owner-occupied LMI buildings only (left), all LMI buildings (right)

From a technical basis alone, there is sufficient rooftop space for at least 33% of LMI consumption to be met with rooftop solar generation. Reaching this potential, however, requires

7

the deployment of models other than those commonly found today, particularly, models that can address coordination issues inherent to rental-occupied and multi-family buildings. Such models must ensure that rental-property owners are incentivized to install solar on their buildings—for example, by bundling utility expenses with rent payments as a means of passing solar costs and savings through to the renter. These models also would need to address the diverging requirements and energy burdens of owners and tenants. For example, California recently developed an incentive program dedicated to affordable multi-family housing, with requirements that at least half of energy generated onsite be used to serve tenants loads (CPUC 2017b). In Colorado, the Denver Housing Authority's 2 MW low-income community solar garden has demonstrated a scalable model for offsite generation through utility partnerships (DOE 2017). Virtual net metering also can be effective in enabling building owners to provide surplus generation directly to their occupants (Feldman et al. 2015).

Technical Potential for Buildings that Serve LMI Populations

Low- and moderate-income households interact with a vast web of non-profit entities, and it is plausible that these buildings could "oversize" photovoltaic (PV) systems on their buildings to share solar generation with their communities. We estimate the generation potential within the cities of Chicago, Illinois; San Bernardino/Riverside, California; and Washington, D.C., for five building types: public sites, public housing, K–12 public schools, homeless shelters, and places of worship. These cities were selected for congruence with a forthcoming companion analysis of the technical, market, regulatory, and social factors affecting LMI solar markets in those three cities. Based on the building's size and average electrical consumption per square foot for comparable buildings, each building's electrical consumption was estimated, and thus the feasibility of oversizing systems to export excess generation to nearby LMI households. Based on these assumption, buildings in Chicago, San Bernardino/Riverside, and Washington, D.C. could feasibly oversize PV systems to provide 2.1%, 8.7%, and 1.3% of LMI consumption, respectively. None of the estimates include on-site ground-mounted systems.

Schools, followed by places of worship had the greatest opportunity to export generation to the community of the five building classes considered. Schools typically have large flat roofs and decrease consumption in the summer, when solar irradiance is highest. Places of worship are favorable because they have low levels of electricity consumption year-round and moderately favorable roof characteristics. Unfortunately, public housing, public sites, and homeless shelters likely have insufficient rooftop space to offset 100% of their own on-site consumption. These results indicate that there is a modest, though not overwhelming, opportunity for buildings that serve LMI populations to oversize a PV system—and that projects are best evaluated on a case-by-case basis.

Conclusions

This report presents a first-of-its-kind assessment of the technical potential of rooftop solar for low- and moderate-income households, as well as providing insight on the distribution of solar potential by tenure, income, and other building characteristics. The findings show that a substantial fraction of the national rooftop solar potential is located on LMI buildings and, for all incomes, a substantial fraction is located on multi-family and renter-occupied buildings. The research also demonstrates that reaching substantial LMI deployment penetration requires deployment on multi-family and renter-occupied buildings. Traditional deployment models have

insufficiently enabled access to solar for these income groups and building types and, without additional innovation either in regulatory, market, or policy arenas, a large fraction of the U.S. potential is unlikely to be met. Potential electric bill savings from rooftop solar would have the greatest material impact on the lives of low-income households as compared to their high-income counterparts and could help mitigate the energy burden faced by these households.

This report ultimately seeks to provide objective data for regulators, policymakers, nonprofits, and project developers to make informed decisions that are best for their own communities. To this effect, data used in this report are provided freely via NREL's website in two formats. One format—an interactive web application using NREL's OpenCarto platform—was developed to enable user to browse, visualize, and export results (https://maps.nrel.gov/solar-for-all). The other format is the Rooftop Energy Potential of Low Income Communities in America (REPLICA) data set (https:/data.nrel.gov/submissions/81) which contains the technical potential data used in this report, accompanied by several additional techno-economic variables (e.g. electricity expenditures ($/month), demographics, utility electric rates) which are available for download as flat files.

Table of Contents

List of Figures

List of Tables

1. Introduction

Residential solar offers a compelling opportunity for reducing the energy burdens faced by low-income households, whose utility bills comprise a larger fraction of expenses than for high-income households. Moreover, because residential solar has disproportionately been adopted by high-income households (Moezzi et al. 2017; Vaishnav et al. 2017), often benefiting from public-funded incentives, it is important to ensure that all utility ratepayers have access to solar benefits including reduced energy burden, increased resilience, and as a hedge against electricity rate changes.

This report seeks to improve understanding of the technical potential of rooftop solar in the residential sector, particularly for low- to moderate- (LMI) income households. Technical potential is a metric that quantifies the maximum generation available from a technology for a given region and does not consider the economic or market viability. This report expands upon previous NREL research investigating the rooftop solar technical potential using light detecting and ranging (LiDAR) scans of individual rooftops in 128 metro regions (Gagnon et al. 2018; Margolis et al. 2017; Gagnon et al. 2016; Phillips and Melius 2016). Using LiDAR scans, as opposed to aerial imagery, allows us to infer the building footprint and the unshaded roof area, azimuth, and tilt for each distinct roof plane. A unique contribution of this work is to estimate rooftop solar technical potential of residential buildings per U.S. Census tract by income, building type, and tenure. To do so, the LiDAR data set is intersected with U.S. Census Bureau socio-demographic and building stock data at the tract-level to better understand how rooftop solar technical potential is allocated among different building types. Statistical techniques also are used to estimate rooftop potential in areas not covered by the LiDAR scans. Collectively, these data and methods enable the study to address three research questions:

1. **What is the quantity and spatial distribution of rooftop technical potential, stratified by income, building type, and tenure?** At a gross level, these data allow improved estimates of the possible opportunity for deployment, as well as the magnitude of various policy interventions.

2. **Among low and moderate-income households, what is the feasibility of achieving parity in solar access across income groups?** Compared to high-income households, LMI households disproportionately live in renter-occupied, multi-family buildings. Because of principal-agent issues in solar adoption, there are significant economic and regulatory barriers inhibiting LMI households from benefiting from the installation of solar on buildings they occupy. Recent U.S. Department of Energy (DOE) solar cost goals could result in solar penetration rates of 17% by 2030 and 33% by 2050 as a fraction of national electricity consumption. This report investigates the feasibility of reaching at least 33% solar penetration for LMI households and, where infeasible, highlights consideration of novel deployment models, such as community solar, virtual net metering, and other shared solar models.

3. Finally, low- and moderate-income households interact with a vast web of nonprofit entities (e.g., churches, schools, public sites, homeless shelters, subsidized housing). **What is the quantity of technical potential for these classes of buildings, and to what extent might these buildings "oversize" systems on their roofs to export generation to LMI households?** Increasing access to solar for such third-parties could either

1

increase their operational efficiency by reducing operational costs, or indirectly provide roof space to households without access.

On a technical basis, the potential for rooftop solar to serve a large fraction of the nation's energy needs is well-recognized (Gagnon et al. 2016; Lopez et al. 2012; Denholm and Margolis 2008; Paidipati et al. 2008; Chaudhari et al. 2004). Rooftops provide a large and sparsely used space to install panels; onsite solar generation can reduce the building's net demand for grid-sourced energy and can reduce losses associated with the distribution and transmission of electricity. Recent analysis has estimated that buildout of *all* suitable roof space could serve approximately 38.6% of U.S. load (Gagnon et al. 2016). This potential is disproportionately located within the residential sector, with small buildings (<5,000 ft^2) contributing nearly 65% of the nation's potential (Gagnon et al. 2016). Previous work, however, has not explicitly considered the intersection of rooftop solar potential with income, building characteristics (e.g., rental versus owner-occupied), and other demographic factors. Though building tenure is not relevant on a technical basis alone, it is very significant from a market perspective.

Adoption of distributed solar in the U.S. residential sector to date primarily has been concentrated among high-income households (Moezzi et al. 2017; Vaishnav et al. 2017). Unlocking technology access and demand from all households could substantially increase market potential—in 2015 43% of all households could be considered to have low to moderate income (<80% area median income(AMI)) and 18% to be middle income (80% to 120% AMI) (U.S. Census 2015). Further, it is not equitable for solar adoption to occur only among high-income households. Recent studies have explored the transfer of wealth implied by technology incentives and net metering policies, finding that majority of public subsidies have been passed through to high-income households (Vaishnav et al. 2017; Borenstein 2017). Without recourse, rooftop solar risks a reputational backlash—in time, it could be perceived as solely the purview of the wealthy, and its deployment not seen as a public benefit.

Ensuring access to affordable energy for all households is a policy mandate for federal, state, and local governments. Costs of energy for low-income households can comprise a substantial fraction of household income and, as a result, many programs exist to ensure its affordability. A notable example is the Low-Income Home Energy Assistance Program (LIHEAP) run by the U.S. Department of Health and Human Services. The program provides financial assistance for home energy bills, energy crises, and weatherization and energy-related minor home repairs (HHS 2017). The U.S. Department of Energy Weatherization Assistance Program also provides assistance for LMI households by increasing the energy efficiency of their homes (DOE 2018). A state-level model is the California Alternate Rates for Energy (CPUC 2017a) program, which gives low-income customers discounts on their electricity and natural gas rates.

As the cost of solar energy continues to decline, many have begun to question what role solar can play in increasing energy affordability or as an efficient alternative or supplemental use of public funds for energy-assistance programs. For instance, use of funds to directly or indirectly incentivize solar deployment might be more cost-efficient than rate subsidization, because it creates a durable asset for low-income households and in the long term could lead to greater program effectiveness. The exact cost-benefit of diverting rate-assistance funds depends on program details and is beyond the scope of this study.

2

Incentivizing solar deployment in LMI communities requires a reimagination of traditional deployment models. These new models should address coordination issues inherent to rental-occupied and multi-family buildings as well as LMI financing and affordability barriers (Cook and Bird 2018). Such models also should ensure that rental-property owners are incentivized to install solar on their buildings, for example, by bundling utility expenses with rent payments as a means of passing savings through to the renter. Alternatively, various shared solar models (Feldman et al. 2015), including virtual net metering, could be effective in allowing building owners to sell rooftop generation directly to the building occupants. Similar issues exist for multi-family buildings, where shared solar or community solar models could help to address tenant-owner coordination issues.

This report ultimately seeks to provide objective data for regulators, policymakers, nonprofits, and project developers to make informed decisions that are best for their own communities; for example, to assess the potential for rooftop solar in their jurisdictions and perform policy cost-benefit analyses. To that end, this report is accompanied by two supporting data products. One is an interactive web application that uses NREL's OpenCarto platform; it was developed to enable users to browse, visualize, and export results (https://maps.nrel.gov/solar-for-all). Another is the technical potential data used in this report—accompanied by several additional techno-economic variables and aggregated at the tract-level—available for download at (https://data.nrel.gov/submissions/81). The Rooftop Energy Potential of Low Income Communities in America (REPLICA) data set includes measures of electricity expenditures ($/month), demographics, utility electric rates, state-level photovoltaic (PV) incentives, measures of environmental quality, and locations of public housing, compiled from a variety of sources and tagged to each Census Tract.

Many opportunities exist to improve the methods used in this report, but there are three important restrictions. One is that the geographic span of LiDAR aerial rooftop imagery is restricted to 128 metro regions, spanning approximately 40% of the U.S. population. A statistical model was developed and validated to estimate potential for unsampled areas, particularly for rural areas. Section 2.2.3 discusses efforts to train and validate this model. Future work could improve the geographic coverage of LiDAR scans in these areas. The second, is that the LiDAR data do not enable the direct observation of the true income, tenure, number of housing units, or income of the building occupants. Instead, these attributes are assigned from tract-level cross-tabulation tables from the 2011–2015 U.S. Census American Community Survey using statistical techniques, including sampling from probability distributions. The final tract-level estimates are based on the median value of a 100-run Monte Carlo process (*see* Appendix B). This sampling process could be greatly improved with access to a national zoning or parcel data set, which would contain a richer set of property-level attributes. Finally, this analysis solely considers the *technical potential* of rooftop solar—or the total solar resource that could be captured given physically-available area and technology performance. Notably, this analysis does not consider the economic or market feasibly of solar installations, nor the feasibly of on-site use of the solar generation.

2. Methods

This section describes the methods used to estimate PV rooftop technical potential by Census tract, stratified by income, building type, and tenure. It includes methods to process LiDAR rooftop scans in the 128 metro regions with coverage (Section 2.1) and estimate their generation productivity (Section 2.1.2). Next, it discusses the intersection of tract-level technical potential and demographic cross-tabulations (Section 2.2.1 and Section 2.2.2). Finally, a statistical model of rooftop potential for the remaining regions of the United States (Section 2.2) is estimated by training it on sampled areas (i.e., those with LiDAR rooftop observations). Additional details on methods are described in the appendices: Allocation of Demographic Attributes (Appendix A); Validation of Monte Carlo Simulations for Building Sampling (Appendix B); Predictive Modeling Framework for Imputing Solar Suitability (C1–C4).

2.1.   Using LiDAR Data to Estimate PV Rooftop Technical Potential

This analysis builds upon previous work pioneered by NREL (Gagnon et al. 2016) using LiDAR data to model rooftop suitability for solar photovoltaics. Light Detection and Ranging (LiDAR) is a remote-sensing method that uses pulsed laser beams to measure distances to the ground. The LiDAR sensing algorithms can be used to infer (1) the presence of individual buildings and their footprint within a city, and (2) the area, tilt, azimuth, and shading of each distinct geometric roof plane on a building's roof. Based on these roof characteristics, the NREL PVWatts (NREL 2017) tool is used to estimate the technical performance for the individual building and thus the collective tract-level building stock.

This work relies on LiDAR data sets provided by the U.S. Department of Homeland Security (DHS) Homeland Security Infrastructure program for 2006–2014. This data set consists of first-return rasters of 1 m^2 resolution and building footprint vectors for 128 metropolitan areas across the nation. Figure 1 shows the metro regions with LiDAR coverage, where the blue polygons are the areas with observed data. In total, this data includes 26.9 million buildings, or about 23% of U.S. buildings (EIA 2013) and covers an area that representing about 40% of the U.S. population.

4
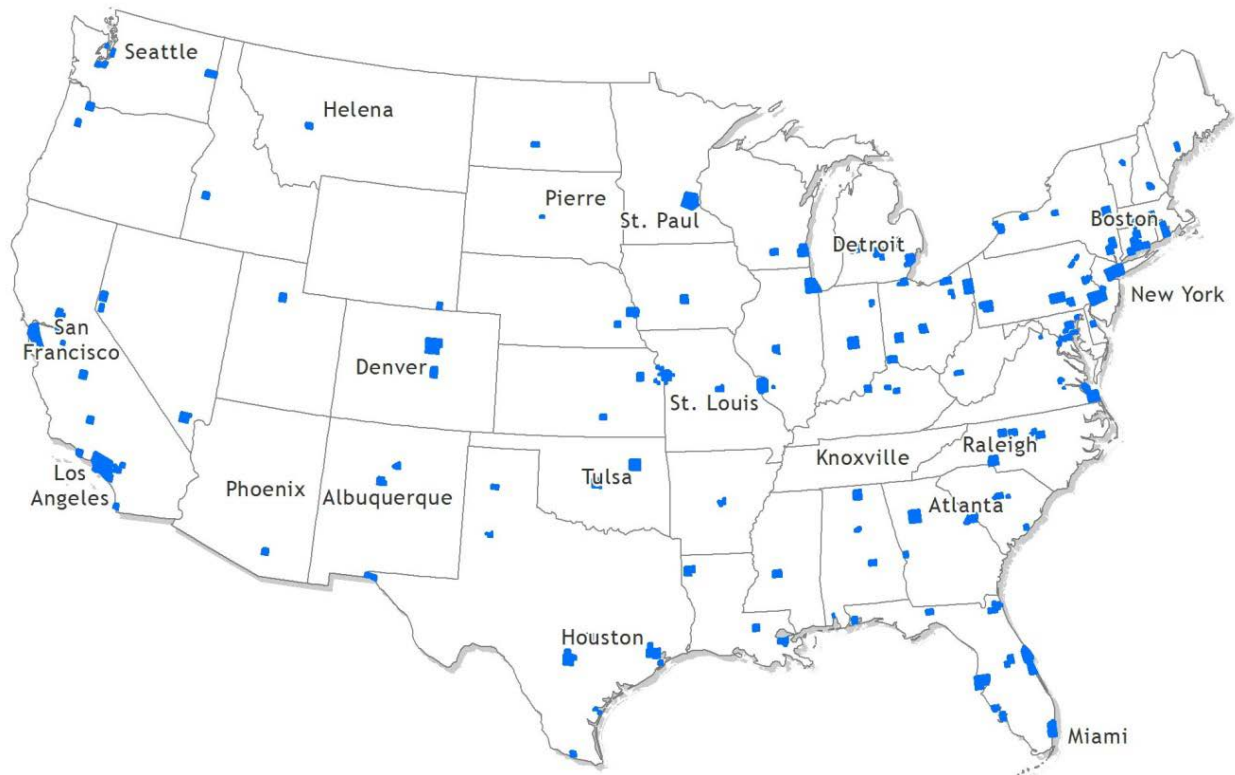
Figure 1. LiDAR data coverage

Using these LiDAR data, Gagnon et al. (2016) developed a geospatial model to identify rooftop planes suitable for rooftop-mounted solar PV given the roof's orientation (tilt and azimuth) and shading characteristics. To account for potential shading from adjacent buildings, trees, or other obstacles, NREL researchers generated hourly hillshades that identify roof square-pixel areas with sufficient sunlight illumination. To identify developable surfaces for PV installment, a zonal mean neighborhood function was used to identify and remove data noise and complex features on roofs (e.g., peaks, edges, chimneys, steeples, facades). Finally, roofs were filtered for rooftop developable surfaces that met basic PV suitability requirements, such as being south-facing and having a minimum area of 10 m^2 (Table 1). The end result is a database of rooftop plane-level data with detailed attribution regarding the slope, tilt, azimuth, installed capacity, and annual generation potential (kWh/year) (discussed in more detail in Section 3.1.2) of all suitable surfaces on all rooftops in the 128 LiDAR–covered metropolitan areas. This data set was an important milestone in the distributed PV field and has paved the way for many subsequent analyses, including the work presented in this report.

5

Table 1. Requirements for Solar Suitable Surfaces

Requirement	Description
Shading	Seasonal requirements[1]: March requires 60% illumination, June requires 70% illumination, September requires 60% illumination, and December requires 50% illumination.
Azimuth	East, Southeast, South, Southwest, or West-facing
Tilt	Average surface tilt <= 60 degree.
Minimum Area[2]	>= 10 m^2

Source: Gagnon et al. (2016).

2.2. Simulating PV Productivity Using reV and PVWatts

Simulations of solar generation were conducted at the tract-level and for 21 tilt-azimuth combinations using the NREL reV tool.[3] The Renewable Energy Potential (reV) model's generation module is a complex wrapper that enables distributed generator performance modeling using NREL's PVWatts model with large renewable resource databases in a parallel computing environment. To simulate PV productivity, reV uses multiple historic solar irradiance time series data from the National Solar Radiation Database (NSRDB), producing generation and capacity factor profiles for a typical meteorological year (TMY). Generation profiles based on TMY data capture hourly variability of an average year and are estimates of the long-term performance of a solar system, though they do not capture significant annual variation in generation due to weather/storm events.

The solar resource and meteorological data used by reV/PVWatts for this analysis are from the National Solar Radiation Database TMY3 data (Wilcox and Marion 2008). These data include hourly representative profiles for 1,001 stations throughout the United States. Each Census Tract is assigned the TMY3 irradiance profile for the weather station closest to the tract's centroid. We also relied on the set of standard technical assumptions used by Gagnon et al. (2016) representing the 2015 average performance of PV systems (Table 2).

---

[1] Seasonal shading requirements, as defined by Gagnon et al. (2016), are used to identify suitable rooftops with adequate percent sunlight illumination throughout the year. Refer to Gagnon et al. (2016) for further details.
[2] Based on current panel power density, 10 m^2 provides sufficient area to install a 1.5 kW system. This minimum area threshold was chosen to represent a conservative lower-end estimate of viable PV system sizes based on current PV performance and historic patterns in reported PV sizing.
[3] Documentation for reV did not exist at the time of writing, but additional information is available at https://www.nrel.gov/gis/modeling.html.

Table 2. Assumptions for PV Performance Simulations

PV System Characteristics	Value for Flat Roofs	Value for Tilted Roofs
Tilt	15 degrees	Midpoint of tilt class
Ratio of module area to roof area[4]	0.70	0.98
Azimuth	180 degrees (south facing)	Midpoint of azimuth class
Module power density	160 W/m^2	
Total system losses	14.08%	
Inverter efficiency	96%	
DC-to-AC ratio[5]	1.2	

Source: Gagnon et al. (2016).

2.3. Estimating National LMI PV Rooftop Technical Potential by Tract

From the LiDAR PV rooftop data set described in Section 2.2, we extend the data set to estimate tract-level solar technical potential by building income, tenure, and building size. This consists of three broad steps: (1) Intersecting individual building technical potential estimates with demographic factors from the Census Bureau 2011–2015 American Community Survey; (2) Aggregating the building-level estimates to the tract, county, and state level and conducting Monte Carlo runs to determine the median estimate; and (3) Training a statistical model on tracts with LiDAR coverage and imputing technical potential for tracts outside of LiDAR coverage.

2.3.1. Estimating Number of LMI Households by Building Type and by Tenure

For the 128 metro regions with LiDAR-derived PV rooftop technical potential, we overlaid demographic data to estimate the total technical potential for residential buildings, per income group, per building type, and per tenure. This work relies on demographic data from the American Community Survey's (ACS) 2011–2015 5-year estimates; see Table 3 for a detailed account on tables used in this analysis. The ACS publishes these data as smaller crosstabs, with much of the detail available only at the larger (i.e., county) geographic levels.[6] To account for this, we use random weighted sampling and proportional allocation methods to disaggregate demographic data into a tract-level cross-tabulation of household counts by AMI income group, per building type and tenure. Additional details on the demographic cross-tabulation process are provided in Appendix A.

---

[4] For flat roofs, the ratio of module area to roof area was assumed to 0.7 to reflect the row spacing necessary to incur only approximately 2.5% losses from self-shading for south-facing modules at a 15-degree tilt. For tilted roofs, the value was assumed to be 0.98 to reflect the 1.27 cm spacing between each module for racking clamps.

[5] A system's direct current to alternating current (DC-to-AC) ratio is the ratio of the nameplate capacity of the PV modules to the AC-rated capacity of the inverters.

[6] Though much of the data is available at the county level, Census Tracts were chosen as the unit of analysis in this report for a few reasons. First, Census Tracts are more homogenous than the larger county and therefore are better areas for delineating between income groupings within a city or region. Second, the underlying LiDAR data is available at the sub-tract level at a 1-meter resolution. Finally, Census Tracts provide a better unit of analysis from a policy and planning perspective, which is the target audience of this report and data.

Table 3. 2015 Five-Year American Community Survey Published Tables Used

Table	Source Code	Universe	Geography
Household Income in the Past 12 Months (in 2015 Inflation-Adjusted Dollars)	B19001	Households	Tract
Tenure by Household Income in the Past 12 Months (in 2015 Inflation-Adjusted Dollars)	B25118	Occupied housing units	County
Tenure by Units in Structure	B25032	Occupied housing units	County
Tenure by Household Size by Units in Structure	B25124	Occupied housing units	County

Source: U.S. Census 2015a, 2015b, 2015c.[7]

This work defines LMI based on the Department of Housing and Urban Development's (HUD) 2016 Area Median Income (AMI) income limits (HUD 2016). These AMI income limits are used to determine the eligibility of applicants for federal assistance programs. They are based off the median income for Fair Market Rent (FMR) areas (i.e., metropolitan areas, parts of some metropolitan areas, and non-metropolitan counties) and are adjusted based on the family size[8] (HUD PD&R). Using these AMI income limits and the generated ACS crosstab described above, we categorize households into the following low- to moderate-income groups, as defined by the Community Development Block Grant (CBDG),[9] based on household income and the number of people in the household:

- Very Low Income: 0% to 30% of AMI[10]

- Low Income: 30% to 50% of AMI

- Moderate Income: 50% to 80% of AMI

- Middle Income: 80% to 120% of AMI

- High Income: >120% of AMI

---

[7] Data extracted using NHGIS (Manson et al. 2017).

[8] The HUD baseline numbers for each income limit are based off the 4-person family size. For households with larger or smaller sizes, percentage adjustments are made to the income break limits based off the number of people in the household (HUD PD&R 2016).

[9] The income categories used in this report are derived from the Community Development Block Grant (CDBG). Though there are many ways in which low- and moderate-income thresholds could be defined, we use the CDBG definition because (1) it includes a class for moderate income, whereas the standard Section-8 definition does not, and (2) it estimates income based on the local geography and the relative cost of living in a particular location. It is important to note that LMI can best be described as a gradient and that delineating between groups does not capture the whole story. Indeed, many assistance programs define "moderate" as a range that extends into what we classify as middle income (up to 120% of AMI) in this report.

[10] The Very-Low Income break limit is based on the greater of the two: (1) 30% AMI or (2) the Federal Poverty Level (FPL), defined by the Department of Health and Human Services (HHS), capped at the low-income limit (50% of AMI) (HUD PD&R 2016). As a result, this leads to fewer households reported in the low-income bin as compared to the very-low income bin. For example, in tracts where the 30% AMI is less than the FPL, the FPL (capped at the low income 50% AMI level) is used as the break limit.

To allocate from ACS income bins to the above income categories we discretize the standard ACS income bins into $1,000 increments and apply the HUD income breakpoints. This allows us to align different ACS crosstabs with different income bins and classify households into the five AMI income groups described above using the AMI breakpoints associated with each household size class. Using a random weighted sampling and proportional allocation approach, we disaggregate county-level tenure and building-type estimates by income group. Further details on these data manipulations and key sampling assumptions are outlined in Appendix A. The result is a data set with total number of households per income group, per building type, and per tenure for all 72,760 tracts in the United States. The next section describes how this data set is joined with solar-generation estimates.

2.3.2. *Estimating LMI Technical Potential for LiDAR Covered Tracts*

We developed a model to estimate the number of occupied residential buildings and gross rooftop technical potential for tracts with LiDAR coverage.[11] In total, LiDAR-covered tracts comprise approximately 32% of the total U.S. Census Tracts. Starting with the demographic crosstab described above, we rely on a series of methods tailored toward translating the counts of households per building type (e.g., single-family detached, 2–4 units, 5+ units) into estimates of building counts by building size class (i.e., small, medium, large). This crosstab ultimately is used to assign building attributes to the individual building IDs from the LiDAR database; LiDAR data alone cannot identify characteristics of building occupants for individual buildings (e.g., residential or not, multi-family or not, low-income or not). To address this challenge, we rely on a few core assumptions and leverage a variety of data to improve the precision of the sampling and allocation process. Note that parcel data—such as property tax assessment—would be a more accurate alternative although no such public data set exists with detailed attribution at a national level.

First, we define a schema of building type to building size (Table 4) to map from building types (e.g., 2- to 4-unit buildings, single family) as reported in the American Community Survey to building sizes in the LiDAR data (e.g., small buildings; 0 to 5,000 ft^2). This schema was derived from the 2009 EIA Residential Energy Consumption Survey (RECS) microdata (EIA 2013), which reports frequencies of total floor space, number of stories, and building types. To estimate the building footprint area, the amount of floor space is divided by the number of building stories. From these calculations, we identified that 99.8% of residential buildings in the United States belong to either the small (< 5,000 ft^2 footprint) or medium (5,000 to 25,000 ft^2 footprint) building classes, 99% of single family buildings are small, 87% of multi-family buildings are small and, 13% are medium. Technical potential for mobile homes is assumed to be null—as the roofs are typically not suitable for solar. These national probabilities are used as weighting factors for sampling residential buildings by building type.

---

[11] Tracts were determined to be covered if there was at least a 90% spatial intersect requirement with the LiDAR extent.

Table 4. Building Type to Building Size Schema

Building Type	Building Size Class[12]	Rooftop Area (ft²)
Single-Family Detached	Small	0 to 5,000 ft²
Single-Family Attached	Small or Medium	0 to 25,000 ft²
Multi-Family 2–4 Units	Small or Medium	0 to 25,000 ft²
Multi-Family 5–19 Units	Small or Medium	0 to 25,000 ft²
Multi-Family 19+ Units	Medium or Large	> 5,001 ft²

Next, we generate a cross-tabulation of possible building count combinations from the ACS household counts by building type (e.g., four housing units in 2- to 4-unit buildings could either be two 2-unit buildings, or one 4-unit building). This array of combinations is narrowed down by removing Census Blocks reported by the HAZUS model[13] (FEMA 2016) to have no residential buildings. We then generate an array of actual building IDs that meet the size criteria of the building-type combinations.[14] In cases where building IDs do not satisfy the criteria of the building-type combinations,[15] we downgrade the building type requirements by the smallest percentage possible. We then bootstrap actual buildings for each building type using our randomly sampled household-to-building count combination as the sampling rate. The sums of the sampled building technical potentials are generated per tract and the income and tenure estimates are stratified using a proportional allocation approach.

The process described above is a stochastic process; the final tract-level and national-level results are determined based on the median of a 100-sample Monte Carlo simulation. The coefficient of variance between samples for each tract and each city were computed for validation purposes, and the tract averages of the 100 runs were calculated. Overall, we found the sampling error to be low, with a mean coefficient of variance of 6.8% and 1.1% for tracts and cities. Further details on the Monte Carlo simulation are covered in Appendix B. The result is a data set of tract-level estimates of suitable buildings and their technical potentials per income group, building type, and tenure for the 37% of U.S. tracts with LiDAR coverage.

These methods rely on a few key assumptions with notable limitations. One is that the proportional allocation approach used to estimate the technical potential by income and tenure assumes that LMI and non-LMI groups (or renter and owner groups) residing in the same building type are equally as likely to be suitable. Suitability in this report is based only on the size, shading, and orientation the roof planes. Other factors such as roof age or roof material, however, are likely to disproportionately affect low-income households and could affect building

---

[12] Small, medium, and large building sizes area convention defined by Gagnon et al. (2016).

[13] HAZUS is a GIS-based natural hazard analysis tool developed by the Federal Emergency Management Agency.

[14] For cases in which the sampling pool of buildings does not satisfy the criteria of the building-type combinations, we downgrade the building-type requirements by the smallest percentage possible.

[15] For any given tract, there are potentially three reasons why the pool of potential residential buildings does not satisfy the building type combinations: (1) the LiDAR data might be outdated (years vary for each city and range from 2006–2014) and new builds could have occurred since the LiDAR scan was collected, (2) the HAZUS General Building Stock reports of residential blocks could be inaccurate or outdated (i.e., residential buildings could exist in blocks reported to only contain non-residential buildings), and (3) the random weighted sampling methodology used in the ACS county-to-tract building type disaggregation might not accurately reflect the building stock in the tract.

solar suitability. Additionally, due to data limitations, the model is unable to identify building occupants' demographics, and this biases intra-tract estimates. That is, although the algorithm does consider inter-tract variance (i.e., smaller homes in low-income tracts), it cannot distinguish intra-tract variance of building size. Notably, we would expect a positive correlation between income and building size or, on a per-capita basis, for owner-occupied buildings to be larger than renter-occupied buildings. These potential biases are offset by the expectation that demographics are mostly homogeneous within a tract because a tract contains about 4,000 people. Another related assumption is that the algorithm does not distinguish between occupants' incomes or tenures living within the same building.

Other limitations of these methods are related to data availability. The lack of access to a national parcel data set that can be used to identify an individual building's true characteristics means that the methods used must rely on FEMA's HAZUS model (FEMA 2016)—a modeled block-level general building stock data set to filter blocks without residential buildings. However, HAZUS itself is an estimated model, and could have zoning inconsistencies. Additionally, the most-recent version of HAZUS is based on data from the 2000 Decennial Census and there might be inconsistencies between residential tracts reported in HAZUS and the 2011–2015 ACS data for tracts with new building construction. Finally, not having parcel data that enables identification of a building's type (i.e., single-family detached, multi-family 2–4 units) and the roof size of different building types, means relying on a schema of building type to building size. This schema of building type to building size (Table 4) is based on data from the 2009 Residential Energy Consumption Survey (RECS) (EIA 2013) to sample buildings for each building type from a pool of LiDAR building footprints based on the building's size. Future work should attempt to use parcel data—including representation of building and roof age—which would permit more-precise identification.

2.3.3. Imputing LMI Technical Potential for Tracts Outside of LiDAR Coverage

To determine the technical potential of the remaining 63% of tracts without LiDAR data we developed a statistical model, trained on the tracts with observed data,[16] to predict tract-level characteristics. The imputation model used largely follows the same methodological framework used in Gagnon et al. (2016, Appendix A–D) but is applied at the tract-level and with additional processes to disambiguate the number and size of buildings from ACS household totals by number of units. This adjusted predictive modeling framework consists of four sub-models, namely:

1. Household-to-Building Model,
2. Small Building Suitability Model,
3. Rooftop Tilt and Azimuth Model, and
4. Rooftop Plane Area Model.

Each model predicts median and upper- and lower-bound estimates for individual components defining the suitable rooftop area. The complete model combines the four component models to estimate median and confidence intervals for tracts without LiDAR coverage. Appendix B details this four-model predictive modeling framework. Coupled with the LiDAR covered tracts

---

[16] Tracts used for the training set were only used if at least 90% of area was covered by the LiDAR raster extent. therefore, weighting of tracts by their coverage is not needed for out-of-sample prediction.

from Section 3.2.2, this provides complete coverage of LMI technical potential across all tracts in the United States.

There are three main limitations with this imputation approach. First, because the LiDAR area estimates for residential buildings are based on the median of sampled runs, the imputation estimates out-of-tract technical potential using modeled inputs. Next, as with the estimates for LiDAR-covered areas, although counts of households by income at the tract-level were available, we do not have direct observations of the cross-tabulation of building income-type-tenure combinations by tract. Instead, these counts are simulated based on the observed proportion at the county level and using income-tenure relationships. In effect, this means that the model does not represent inter-tract differences in proportion of, for example, rental versus owner-occupied buildings within the county. Third, imputed results for rural areas likely are biased because most of the observed LiDAR data is in urban areas. This bias is mitigated, however, by use of urban-rural isolating variables as independent variables (i.e., locale and land use and land cover) in our predictive modeling.

2.4. Model Uncertainty and Caution in Interpreting Results

Results presented in this report are based on a series of statistical processes, often with varying degrees of certainty. For reasons described below, this report is unable to provide 95% confidence intervals for all of the estimates, although the authors acknowledge this unintentionally could overstate the certainty of the results. Thus, readers are urged to use caution when interpreting results—particularly for policy-planning or regulatory considerations. Two dimensions of uncertainty within the data are highlighted.

2.4.1 Uncertainty of solar potential for LiDAR-covered and non-covered areas.

The primary data used in this report are a series of LiDAR scans of individual buildings for 128 metro regions, spanning 40% of the U.S. population. For these regions the LiDAR data enables the accurate assessment of the total number of buildings in the tract, their area, and the fraction of buildings with solar-suitable roofs (solar suitability). Summing over all the buildings gives a high degree of confidence of the total residential potential in these tracts. Assigning these buildings to the residential sector, estimates of the ratio of the number of buildings per building type, and estimates of building size to building type also makes assumptions documented in the Methods section. The process uses several sub-models, and the estimates do not have a composite confidence internal because the data required to quantify the composite error is unavailable. We were able to quantify the error of the LiDAR-covered areas in an indirect way, however, by rerunning the model 100 times with different random seeds. When doing so, we found that the average tract-level estimates had a coefficient of variance of 6.8%. That is, the standard deviation of the 100 runs was 6.8% of the mean estimate. For cities, which are composed of several tracts, the mean coefficient of variance was 1.1%. Both statistics give assurance that the error of the various sampling methods is acceptably low.

We then trained statistical models to impute the gross solar potential for the building stock in each non-LiDAR tract. By its nature, this statistical process is less accurate than having directly-observed data. The imputation process uses sub-models to individually estimate the ratio of households to buildings, the fraction of solar-suitable buildings, the distribution of rooftop tilts and azimuths, and the distribution of rooftop plane areas. Because we don't have direct

12

observations of rooftops in the non-LiDAR covered areas we are not able to directly estimate the error. However, we did validate the statistical model by training it on 75% of the LiDAR-covered areas, to test its accuracy when applied to the remaining 25%. Comparing the gross predicted LMI technical potential for the tract to the actual value shows that 68% of the estimates are within 10% of the actual values and 90% of the predicted values are within 20% of actual values. Tract-level variance of this magnitude could be unacceptable for planning purposes, although the accuracy increases when moving to sequentially larger geographic areas (cities, counties, states).

2.4.1 Uncertainty of distribution of solar potential by income-tenure-types

A key purpose of this report is to estimate solar technical potential for different income-tenure-type combinations (e.g. 50% to 80% AMI, owner-occupied single-family buildings). The LiDAR data does not allow us to directly observe the zoning, income level, tenure, or building type of individual buildings. To estimate the frequency of these different combinations for tracts with LiDAR coverage, the LiDAR data is intersected with various Census American Community Survey data. The justification is that, although the estimate of income-tenure-type for any individual building cannot be estimated, the accuracy at a tract or county level improves when averaged over thousands of buildings. For tracts with hundreds of buildings or fewer, then this source of error could be greater.

Another important note is that the Census does not publish direct observations of income-tenure-type counts at the tract-level. Instead, the estimates herein are compiled from a variety of sources. At the tract-level, there is observed data on the count of households by income group. Cross-tabulations of tenure by income, however, and tenure by household size by housing units in a building all are observed at the county level. To disaggregate to the tract level, we used proportions of income at the tract level to proportionally disaggregate the income-tenure counts from the county. These estimates could be biased whenever a specific tract has substantially different proportions of income-tenure-housing type combinations than the county does. For this reason, income-tenure tract combinations only are presented in tabular results at the national level, where the bias should be minimized by aggregation. In the interest of transparency, however, these values are presented at the tract level in the Solar for All web application and the REPLICA data set with appropriate disclosure.

3. Results

This section quantifies the technical potential of roof-mounted solar photovoltaic systems, stratified by the income of the building occupants, tenure, and size of the building. In particular, this report provides two novel contributions. One is that it estimates the intersection of rooftop potential with the above building demographics. Another is that the data is aggregated at the U.S. tract and county-level, instead of by zip code, which is more congruent with Census Bureau, HUD, and other socio-demographic analyses. In Section 3.1 the quantity and spatial distribution of rooftop technical potential across various building characteristics is estimated. In 3.2 the feasibility of rooftop solar offsetting 33% of residential electricity consumption is explored, with a focus on the feasibility of reaching parity in adoption levels across income. Finally, in Section 3.3, the report diverges from a national analysis to explore the rooftop technical potential in more depth in Chicago, Illinois; San Bernardino/Riverside, California; and Washington, D.C., to understand the spatial distribution of potential within these cities as well as the potential on non-residential buildings that serve low-income populations.

3.1. National Residential Rooftop PV Technical Potential

Over all tracts and all residential buildings in the United States, the gross annual residential rooftop solar technical potential is nearly 1,000 TWh, or about 75% of residential consumption (DOE EERE 2017). Significant potential is found in every income group (Table 5), with the greatest overall potential in the non-LMI income group, and with 416 TWh for low-to-moderate (0% to 80% AMI) households over 25.5 million solar-suitable buildings. The LMI opportunity is approximately 42% of the total U.S. residential potential, indicating that it is a non-trivial portion of the suitable rooftop space. These estimates should be interpreted as the gross technical potential of all residential buildings, i.e. they do not consider existing residential PV; in 2016, approximately 1% of residential buildings have installed rooftop PV (EIA 2017).

The gross technical potential by income group was primarily proportional to the number of buildings, though there are differences on a per-capita basis between the groups. Nationally, the average technical potential was 14,878 kWh per building. However, the per-building technical potential is inversely associated with income (17,106 to 13,711 kWh per building for Very Low to High) because of the higher rate of occupancy in multi-family buildings among LMI households, which tend to have larger, flatter roofs than their single-family counterparts. On a per-household basis, however, the technical potential is positively correlated with income because the same multi-family buildings have higher household-to-roof area ratios (8,246 to 8,763kWh per household for Very Low to High; 8,553 kWh per household nationally). Taken together, these results demonstrate that there is significant per-capita technical potential for all income groups, although—as is demonstrated in Section 3.1.2—much of the LMI potential is sited on rental-occupied and multi-family buildings.

14

Table 5. National Residential PV Rooftop Technical Potential by Income Group

Income Group		Households (millions)	Suitable Buildings (millions)	Suitable Module Area (millions of m²)	Capacity Potential (GW$_{DC}$)	Annual Generation Potential (TWh/year)
LMI—	Very Low (0%–30% AMI)	19.5	9.4	794.4	127.1	160.8
	Low (30%–50% AMI)	11.5	5.7	472.8	75.6	95.3
	Moderate (50%–80% AMI)	18.8	10.4	792.0	126.7	159.8
Non-LMI	Middle (80%–120% AMI)	21.1	12.3	900.4	144.1	180.8
	High (> 120% AMI)	46.0	29.4	2,003.3	320.5	403.1
All LMI Buildings		49.8	25.5	2,059.2	329.4	415.9
All Residential Buildings		116.9	67.2	4,962.9	794.0	999.8

These estimates are congruent with previous estimates of the total U.S. rooftop technical potential, though none of the previous studies explicitly estimate the distribution among income, building types, and tenures. Gagnon et al. (2016), for instance, estimated 1,432 TWh of rooftop potential across small, medium, and large building types and 926 TWh for small buildings only. Differences between the results presented in this report and those presented in Gagnon et al. (2016) can be attributed to differences in scope. Specifically, this report seeks to estimate the total *residential* technical potential, whereas the previous work estimates potential by building size class (i.e., small, medium, large). Most small buildings are single-family residential (94%) (Gagnon et al. 2016), though not all residential buildings are small; 13% of multi-family residential buildings are medium or large (EIA 2013). Thus, the estimate for the residential sector (999.8 TWh) is a mixture of the Gagnon et al. (2016) estimates of small (926 TWh) and medium and large buildings (506 TWh). In contrast, Denholm and Margolis (2008) estimated 419 TWh for the residential sector, though this study relied on coarser methods. Additionally, these technical potential estimates only include roof-mounted systems on residential buildings; for context, previous estimates of the technical potential for ground-mounted systems are vastly larger (281,000 TWh) due to the greater area available for deployment (Lopez et al. 2012).

3.1.1. Spatial Trends in LMI Technical Potential

Figure 2 demonstrates the overall quantity of residential potential by U.S. county in gigawatt-hours. We find that the quantity of technical potential is highly concentrated amid urban and other densely-populated areas with more building stock. Many of the areas with high levels of potential already have significant levels of residential solar deployment (e.g. Arizona, California,

Maryland, Massachusetts, New Jersey), although there also are several states with high solar potential with currently-low levels of solar deployment (e.g. Illinois, Ohio, Florida, Pennsylvania, Texas) (GTM 2017)—indicating the opportunity for future growth.
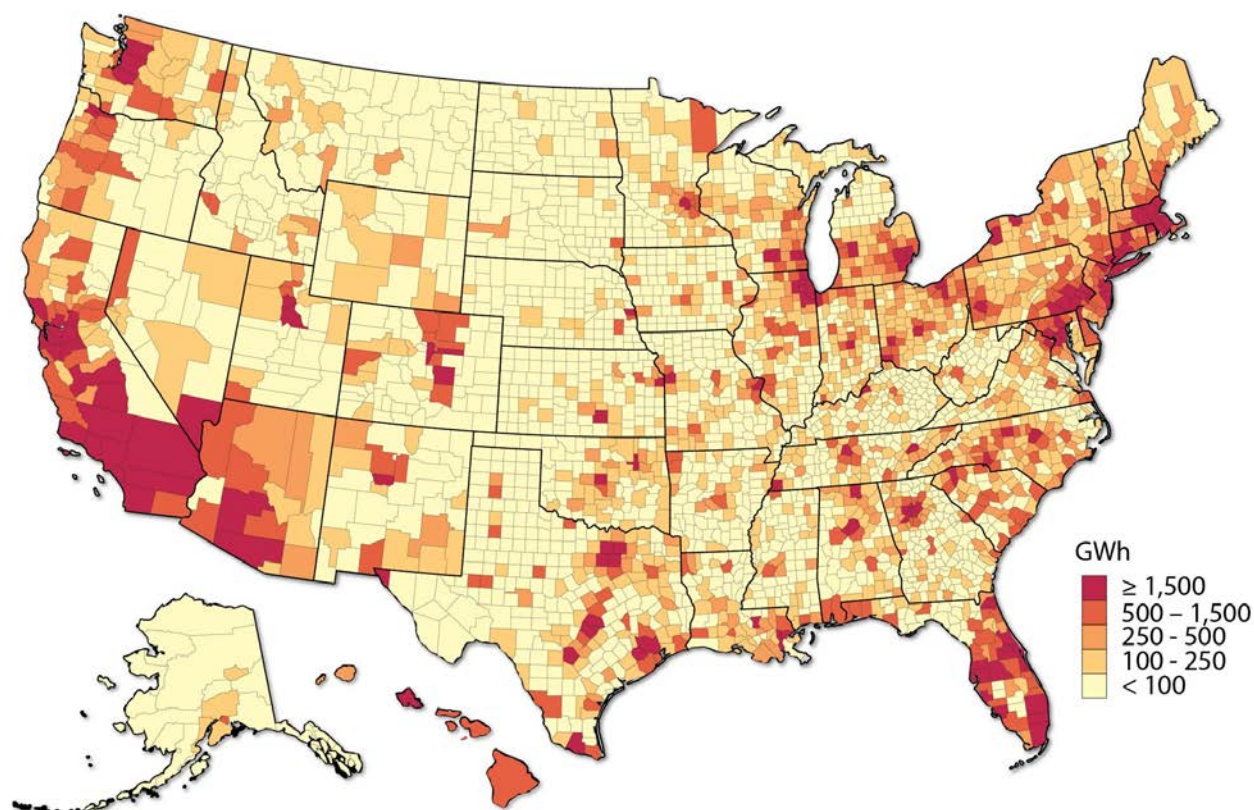
Figure 2. County residential technical potential (GWh)

Figure 3 shows the county-level technical potential, normalized as the percent of county residential generation potential provided by LMI-occupied buildings. Compared to Figure 2— which demonstrates the areas with the greatest overall LMI potential—Figure 3 shows areas with disproportionately high LMI potential after normalizing for population. We find that in 437 counties (14%) LMI technical potential comprises at least half of the county's rooftop solar potential. Spatial trends in the fraction of LMI potential are substantially different than those of the absolute amount. At a high-level, patterns of LMI potential mirror overall income trends in the United States. LMI potential percentages are greatest in lower-income counties and are also distinctly higher in rural or semi-rural counties. Areas with disproportionately greater fractions of LMI potential are seen in the Southeast (i.e., Alabama, Arkansas, Kentucky, Louisiana, Mississippi, West Virginia) and portions of Midwest and Mountain West.

16
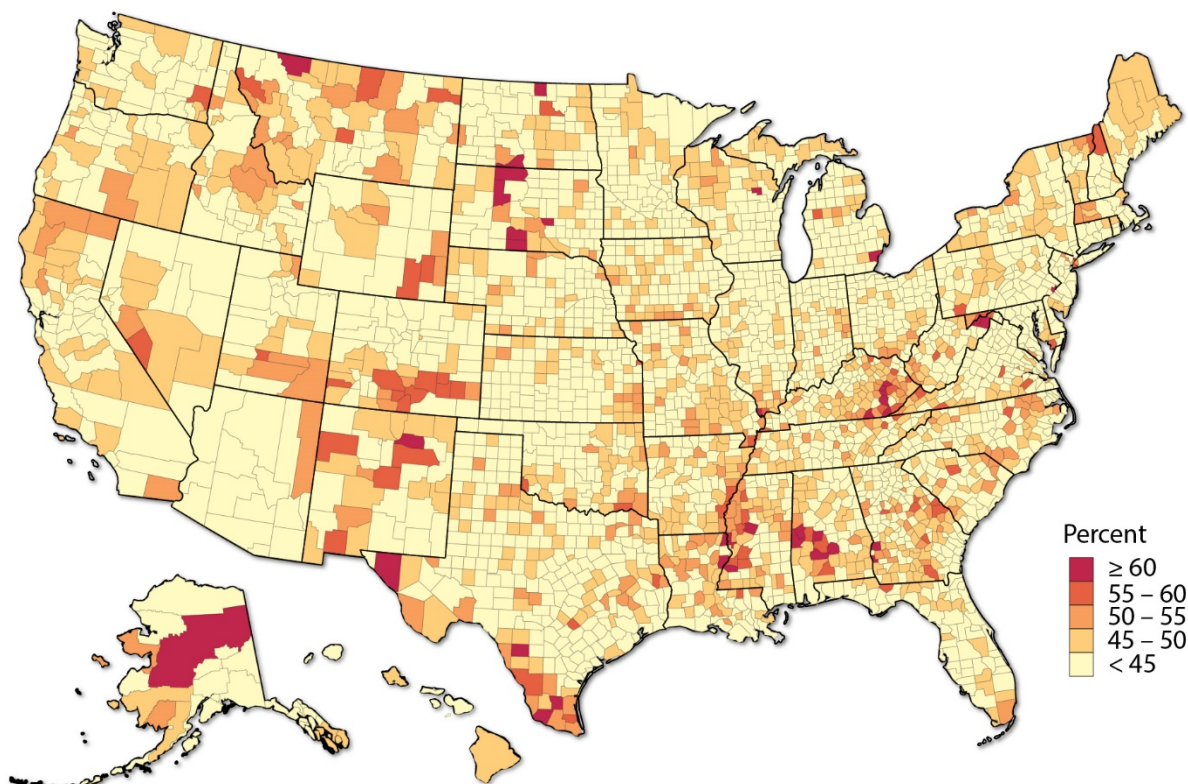
Figure 3. County LMI rooftop technical potential as percent of total residential potential

Previous national maps (i.e., Figure 2, Figure 3) are represented at the county-level, though the underlying data is tract-level, because tract-level maps are too finely resolved to show meaningful spatial trends at a national scale. Tract-level maps, however, are well-suited to demonstrate community-level patterns within a city. As a demonstration we mapped solar technical potential for LMI households at the tract level for four cities—Chicago, Illinois; San Bernardino/Riverside, California; and Washington, D.C. (Figure 4), normalized by the tract's total residential generation potential. These cities were selected for congruence with a forthcoming companion analysis of the technical, market, regulatory, and social factors affecting LMI solar markets in those three cities. Unsurprisingly, LMI generation is strongly correlated with lower-income neighborhoods in each city. Moreover, the results demonstrate that a substantial portion of each city's solar technical potential is in LMI neighborhoods. Therefore, lower deployment of solar in lower-income neighborhoods would substantially limit the overall deployment potential in these cities.

For additional analysis opportunities at the city-level, readers are invited to explore the accompanying web app (https://maps.nrel.gov/solar-for-all), which can be used to explore additional dimensions of the underlying data.
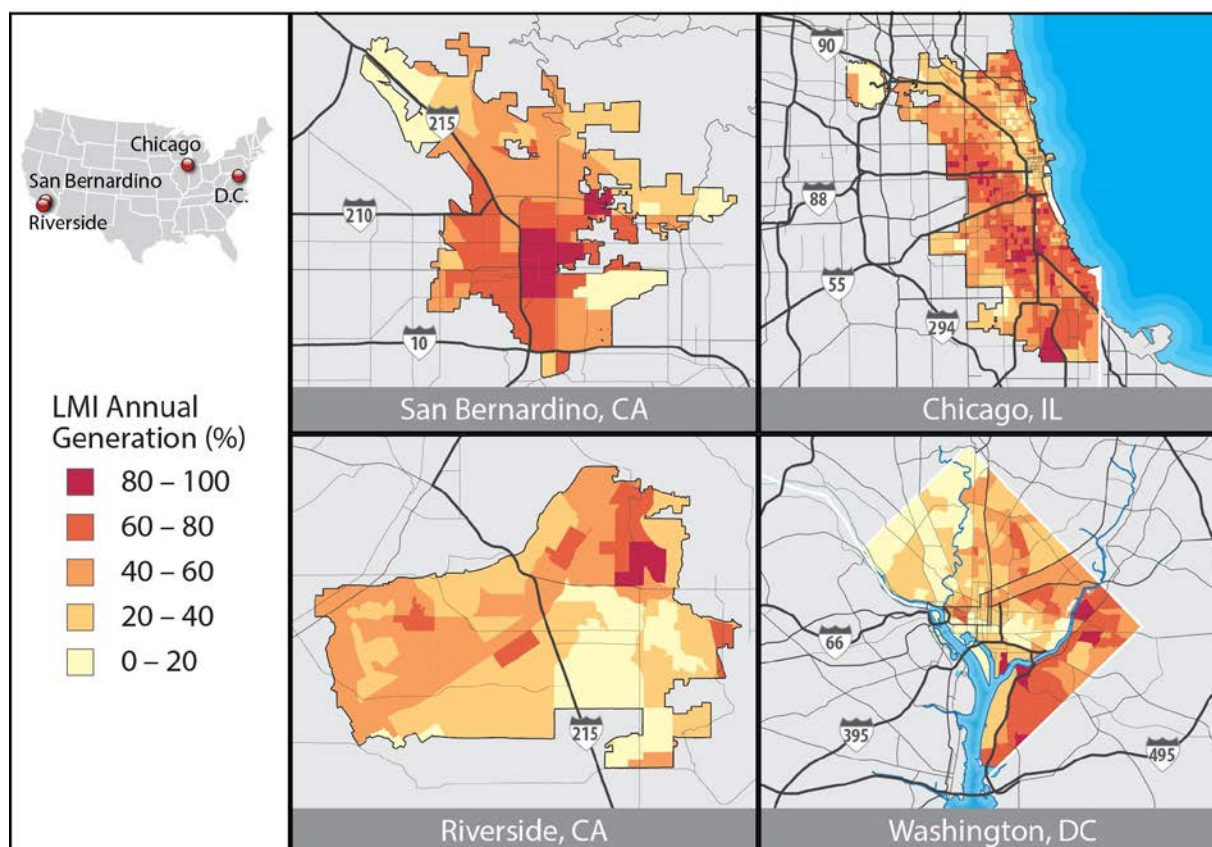
Figure 4. Percentage of tract-level rooftop solar potential (MW) on LMI buildings

3.1.2. Technical Potential by Tenure, Building Type, and Income

This section discusses a first-of-kind estimate of the distribution of rooftop PV technical potential by building tenure, housing unit type, and income in the U.S. residential sector. The current U.S. residential rooftop PV market largely is concentrated among high-income households and for single-family owner-occupied homes (Moezzi et al. 2017; Vaishnav et al. 2017). Solar deployment on renter-occupied buildings is low because of principal-agent issues in the motivation for building owners to install solar. Namely, because most tenants (88%) directly pay for their utility expenses (EIA 2013), there is reduced incentive for building owners to invest in solar or other building improvements. Building owners need reasonable confidence that these investments could be recouped through higher rent payments, which could be untenable for affordable housing. Similar coordination issues exist for multi-family buildings. LMI households face other unique barriers to solar adoption, including limited access to financing and available funds (Cook and Bird 2017). If unresolved through policy, market, or regulatory measures, these coordination and financing issues will inhibit solar deployment on a large fraction of the U.S. building stock.

Figure 5 illustrates the distribution of generation potential by income group and building type. We estimate that a majority of the residential potential (683 TWh, 68.4%) is situated on single-family buildings, as compared to multi-family buildings (316 TWh, 31.6%) and single-family potential exceeded multi-family potential for each income group. Within LMI households, however, the distribution is more uniform, with multi-family buildings comprising 40.1% of the LMI-specific potential.
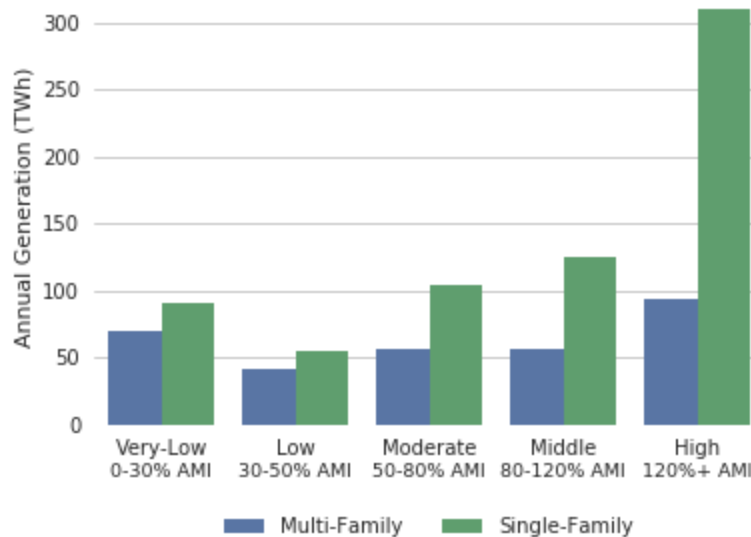
Figure 5. Generation potential by income group and building type

Similar trends are seen for the segmentation of potential between owner-occupied and renter-occupied buildings (Figure 6) as there is a strong correlation between occupancy in multi-family buildings and rental status. We estimate that 659 TWh (65.9% of the residential potential) is situated on owner-occupied buildings, as compared to 341 TWh for renter-occupied buildings (34.1%). For LMI households, potential on renter-occupied buildings (212.7 TWh) slightly exceeds that of LMI owner-occupied buildings (203.3 TWh).
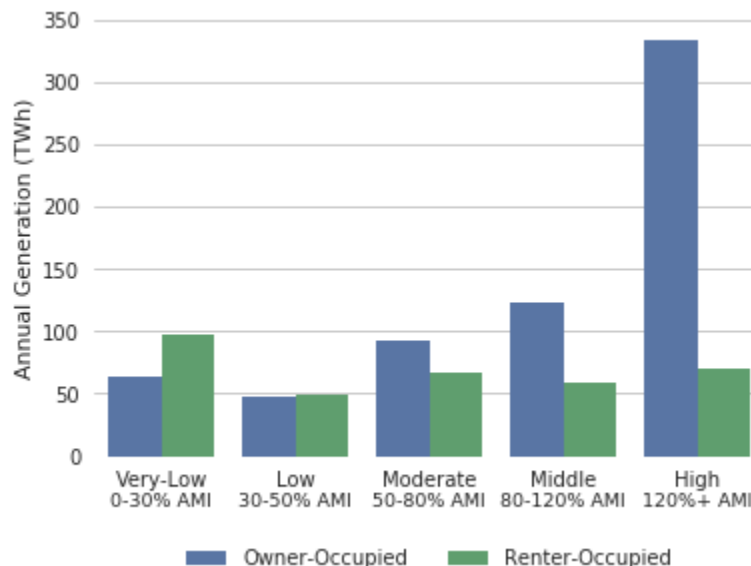
Figure 6. Generation potential by income group and building tenure

Taken together, Figure 7 shows the intersection of potential by both tenure and building type for LMI families. The largest modality of potential is for single-family owner-occupied buildings (176.8 TWh), followed closely by multi-family renter-occupied buildings (140.1 TWh). Though deployment of rooftop solar historically has been concentrated on single-family, owner-occupied

19

buildings, these results indicate that nearly 60% of potential for LMI buildings exists on these other underrecognized tenure-type combinations. Table 6 shows the national technical potential estimates for all income-tenure-type combinations.
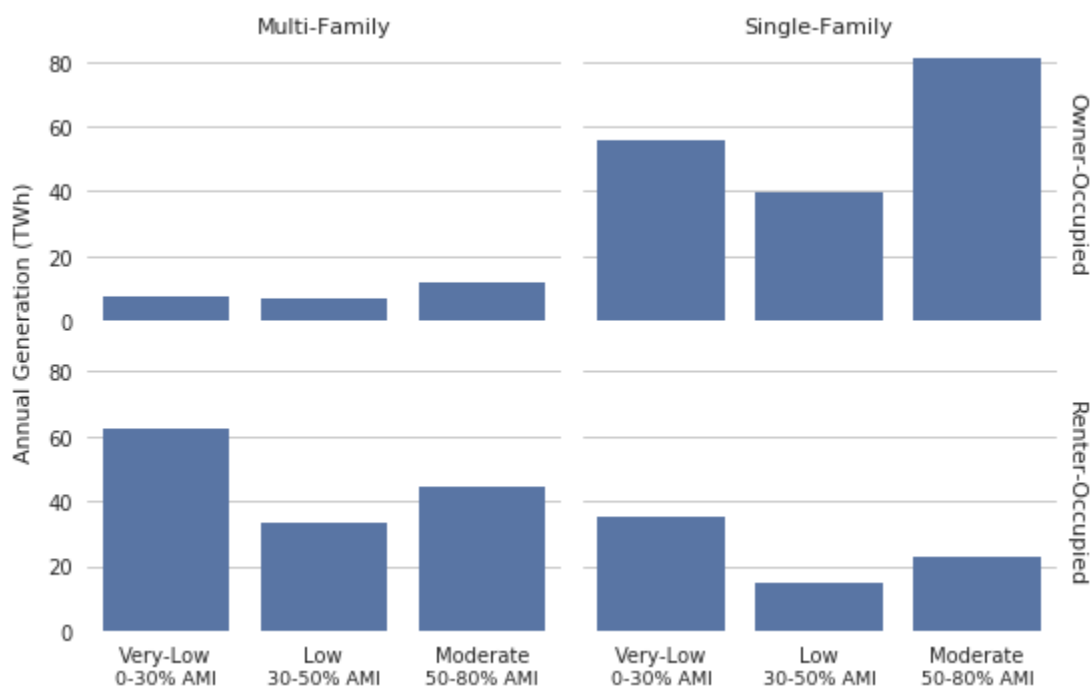
Figure 7. Generation potential (TWh) by building type and tenure

Table 6. National residential PV rooftop technical potential by income group

Income Group	Tenure	Building Type	Suitable Buildings (millions)	Suitable Module Area (millions of m^2)	Capacity Potential (GW$_{DC}$)	Annual Generation Potential (TWh/year)
Very Low (0%–30% AMI)	Owner-Occupied	Multi-Family	0.1	38.3	6.1	7.8
		Single-Family	5.1	274.7	43.9	55.7
	Renter-Occupied	Multi-Family	1.0	311.8	49.9	62.4
		Single-Family	3.1	169.5	27.1	34.9
Low (30%–50% AMI)	Owner-Occupied	Multi-Family	0.1	34.2	5.5	6.9
		Single-Family	3.7	198.3	31.7	40.0
	Renter-Occupied	Multi-Family	0.6	168.0	26.9	33.6
		Single-Family	1.3	72.3	11.6	14.9
Moderate (50%–80% AMI)	Owner-Occupied	Multi-Family	0.2	59.6	9.5	11.9
		Single-Family	7.4	402.7	64.4	81.1
	Renter-Occupied	Multi-Family	0.7	219.9	35.2	44.1
		Single-Family	2.0	109.9	17.6	22.7
Middle (80%–120% AMI)	Owner-Occupied	Multi-Family	0.3	84.2	13.5	16.7
		Single-Family	9.7	527.6	84.4	105.8
	Renter-Occupied	Multi-Family	0.6	196.4	31.4	39.3
		Single-Family	1.7	92.2	14.7	19.1
High (>120% AMI)	Owner-Occupied	Multi-Family	0.8	234.2	37.5	46.2
		Single-Family	25.9	1424.7	227.9	286.8
	Renter-Occupied	Multi-Family	0.8	237.7	38.0	47.8

Single-Family	1.9	106.8	17.1	22.3

3.2. Feasibility of Parity in Solar Adoption Rates

The U.S. Department of Energy Solar Energy Technology Office recently announced updated cost targets for solar energy of $0.05/kWh for residential-scale solar systems by 2030. Using the Regional Energy Deployment System (ReEDS) capacity expansion model, NREL estimated that achieving these costs could result in 405 GW of PV capacity in 2030, which would provide 17% of contiguous U.S. electricity generation (Cole et al. 2017). By 2050, deployment could increase to 971 GW, which would provide 33% of generation. These projections do not explicitly delineate between utility-scale and distributed-scale solar, nor do they impose constraints of minimum regional penetration levels.

This report investigates the technical feasibility of reaching parity in adoption rates of distributed solar in the residential sector, regardless of socioeconomic status. Because of the ambiguity of the announced goals, the authors interpret this to mean, "Is there sufficient technical potential for rooftop solar to offset 33% of low- and moderate-income household annual electrical consumption in each U.S. county?" In counties where technical or market barriers prevent reaching the consumption-offset goal, we also investigate what types of new business models would be required, such as community solar, or virtual net metering (Feldman et al. 2015; Cook and Bird 2018).

To assess the viability of the consumption offset targets we first estimated the total electric consumption of low- and moderate-income households aggregated by county. To do so, we start with the Low-Income Energy Affordability Data (LEAD) residential energy expenditure data set which estimates average annual energy expenditures per Census tract, AMI income group,[17] tenure, and building type (among other breakdowns) (DOE EERE 2017). The LEAD data set is based off the 2011–2015 American Community Survey Public Use Microdata Samples (PUMS) of self-reported monthly household electricity expenditures. Using this data, the yearly household expenditure[18] is divided by the average cost of electricity per tract,[19] to get the per-household yearly electrical consumption at the tract level. This number then is multiplied by the number of households in the tract to derive the total residential energy consumption by tract. Due to high variability within the expenditure data at the tract level, we aggregate these results to the county level to gain more confidence in the results.[20] Table 6 demonstrates key national statistics

---

[17] Note that due differences in the way the AMI incomes are grouped in the LEAD data, we are unable to separately identify electrical consumption for the 'Middle' (i.e., 80%–120% AMI) and High (i.e., 120%+) income groups, so they are reported combined as "Non-LMI" (i.e., 80%+) in this section of the report.

[18] A slight mismatch exists when aligning the LEAD data with the data from the present research. This mismatch is due to differences in disaggregation methods used for each analysis. Though the mismatch is minimal, there are tract instances where LEAD reports no households (of a building type, tenure, and income group) where we report household counts. These instances use the state averages of LEAD energy expenditures, per group, to backfill the data.

[19] Average cost of electricity per tract was calculated using the 2016 EIA 861 (EIA 2016b) utility survey reporting total kilowatt-hours sold divided by the number of customers served, per utility and state, for bundled utilities only. Tracts were geospatially tagged to each utility territory using Ventyx ABB electric utility territory geometries (ABB Energy 2017) and ties were broken using NREL's standard methodology. In cases where no data was reported by the EIA 861 for a tract, the state average was used.

[20] Validations of LEAD data were performed at the aggregate by comparing national results to RECS estimates. The RECS data is insufficiently resolved to permit comparison at the tract or county level.

of residential energy consumption, where the total residential annual consumption is estimated at 1,325 TWh and the consumption for LMI (0%–80% AMI) households is estimated at 493 TWh.

Table 7. Annual Residential Electricity Consumption by Income, Building Tenure, and Type

Income Group	Building Tenure	Building Type	Annual Electricity Consumption (TWh)
Very Low (0%–30% AMI)	Owner-Occupied	Multi-Family	1.1
		Other	8.0
		Single-Family	76.6
	Rental-Occupied	Multi-Family	41.7
		Other	8.2
		Single-Family	52.6
Low (30%–50% AMI)	Owner-Occupied	Multi-Family	1.6
		Other	3.6
		Single-Family	51.4
	Rental-Occupied	Multi-Family	23.5
		Other	2.6
		Single-Family	21.1
Moderate (50%–80% AMI)	Owner-Occupied	Multi-Family	3.0
		Other	10.3
		Single-Family	113.9
	Rental-Occupied	Multi-Family	32.7
		Other	5.3
		Single-Family	35.3
Non-LMI (80%+ AMI)	Owner-Occupied	Multi-Family	19.8
		Other	47.9
		Single-Family	620.2
	Rental-Occupied	Multi-Family	67.9
		Other	9.3
		Single-Family	67.0
Total LMI			492.7
Total Residential			1324.6

Income Group	Building Tenure	Building Type	Annual Electricity Consumption (TWh)
Very Low (0%–30% AMI)	Owner-Occupied	Multi-Family	1.1
		Other	8.0
		Single-Family	76.6
	Rental-Occupied	Multi-Family	41.7
		Other	8.2

The method of matching generation potential to household consumption makes three assumptions. First, because the LiDAR data does not enable the identification of consumption at the individual-building level, the analysis does not explicitly consider mismatches of generation potential and consumption at the individual household level, only in aggregate at the county level. Multiple factors explain variance in household electrical consumption (e.g., number of occupants, building efficiency, fuels used for heating) as well as variance in the building-level solar suitability (e.g., unshaded roof area, tilt, azimuth). Next, use of the average cost of electricity could underestimate the electrical consumption since some utilities offer below-market electricity rates for low-income and elderly subscribers. Despite this potential bias, average electrical rates were used because a county-level database of low-income rates was not available. Finally, although use of fuels such as natural gas and fuel oil are a significant portion of energy expenditures for some households, the present work only considers offsetting existing electrical consumption; considering the electrification of these end uses is beyond the scope of this study.

Using these techniques, Figure 8 compares estimates of the solar technical potential with electrical consumption by income group, for the single-family owner-occupied (SFOO) building stock only. We start with this intentionally conservative comparison because, as described earlier, there are currently significant barriers to deploying residential solar on renter-occupied and multi-family buildings. Under this assumption we find that offsetting at least 33% of LMI electrical consumption with rooftop solar only on SFOO buildings is technically feasible on a national scale for all income groups except the Very-Low (0% to 30% AMI) group. However, this feasibility belies a few practicalities. First, it implies buildout of nearly all SFOO roof space—an impractical and unforgiving market challenge. Second, deployment on SFOO buildings alone implies that residents of renter-occupied and multi-family buildings would not be served, counter to the goal of increasing widespread solar access. Notably, the fraction of consumption that can be offset with SFOO buildings is inversely correlated with income group because of lower occupancy in SFOO by LMI households. This means that deployment on SFOO-only buildings leads to lower consumption-offset levels for the lowest-income households. We note that these calculations exclude the effects of roof age or measures needed to improve roof structural suitability as these were classified as economic, rather than technical, factors.

24
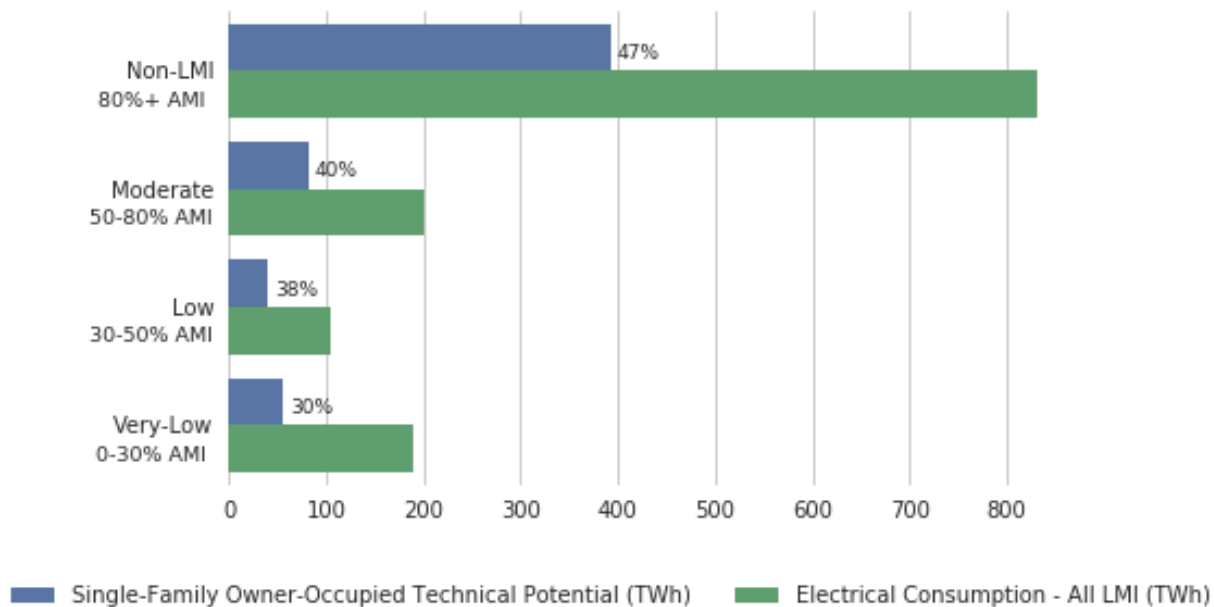
Figure 8. Comparison of fraction of consumption met by generation potential for single-family owner-occupied buildings alone, by income group

Next, we estimate the feasibility of solar consumption offset targets when considering the entire residential building stock. We find that there is more than sufficient roof space, on a technical basis, to offset 33% of LMI electricity consumption, although to do so would require deployment on rental-occupied and multi-family buildings. Deployment on these classes of buildings likely would require development of new business models or other regulatory changes. Figure 9 demonstrates the combined national technical potential for the four tenure-type combinations, single-family owner-occupied (SFOO), single-family renter-occupied (SFRO), multi-family owner-occupied (MFOO), and multi-family renter-occupied (MFRO), as compared to the electricity consumed for each group, both on a national basis. For the Very Low, Low, Moderate, and Non-LMI income groups the percent of generation potential to electrical consumption is 85%, 91%, 80%, and 70%, respectively. Due to lower per-capita levels of consumption for low-income households, the fraction of consumption that can be offset is greater for LMI households than for non-LMI households. Note that none of the income groups are projected to have a technical potential that *exceeds* the group's consumption level.

25
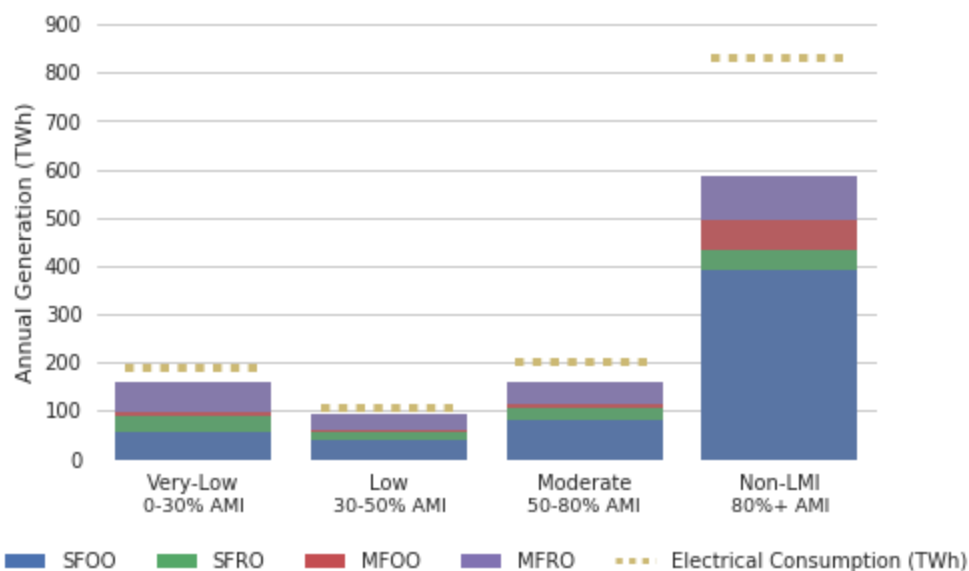
Figure 9. Technical feasibility of matching residential electrical consumption with rooftop solar, by income group

- Though there is sufficient roof space on a national basis to offset 33% of electricity consumed for LMI buildings, the roof space is insufficient in all counties. Table 8 demonstrates, on a national basis, the sum of the discrepancy between generation potential and a 33% offset for each building type for LMI households. Shortfalls are most significant for mobile homes (38 TWh)—whose roofs are typically not structurally suitable for solar, followed by single-family (6 TWh) and multi-family (2 TWh) buildings. Therefore, many occupants of mobile homes—who are disproportionately low-income—face significant challenges in gaining access to solar energy.

Table 8. Estimates of National Shortfall in Rooftop Solar Generation Needed to Nationally Offset 17% and 33% of LMI Consumption

Goal	Building Type	GWh Needed
17%	Multi-Family	789.9
	Single-Family	1,224.8
	Other[21]	38,026.8
33%	Multi-Family	1,905.2
	Single-Family	6,085.5
	Other	38,026.8

---

[21] "Other" building types primarily include mobile homes, but also include other miscellaneous residential electricity uses (e.g., boats, recreation vehicles).

26

Figure 10 shows the maximum ratio of LMI electrical consumption that could be offset with rooftop solar from all LMI buildings in the county. When allowing deployment on LMI rental-occupied and multi-family buildings, there are 31 counties with insufficient technical potential to offset at least 33% electrical consumption, or about 3 TWh shortfall. When allowing deployment only on single-family owner-occupied LMI buildings (Figure 11), however, there are 1,257 counties (40% of all U.S. counties) with insufficient potential to reach at least 33% consumption offset, or about 202 TWh shortfall. Again, note that the statistics in Figure 10 and Figure 11 represent the *average* penetration achievable for the entire building stock in the county; there are likely to be significant variance in the achievable penetration for individual buildings based on the roof characteristics and occupants' energy use.

Spatial trends in generation penetration largely mirror regional variation in per-capita electricity consumed, primarily due to which fuels are used for building heating and cooling loads. For instance, per capita electricity consumption is greater in the Southeast because electricity is the predominant fuel for heating and cooling loads in that region, whereas natural gas is the predominant fuel in California and Southwest, and fuel oil is predominant for the Northeast. In effect, this means that more solar generation is needed to offset the 33% of consumption in the Southeast, but less is required in California, the Southwest, and the Northeast.
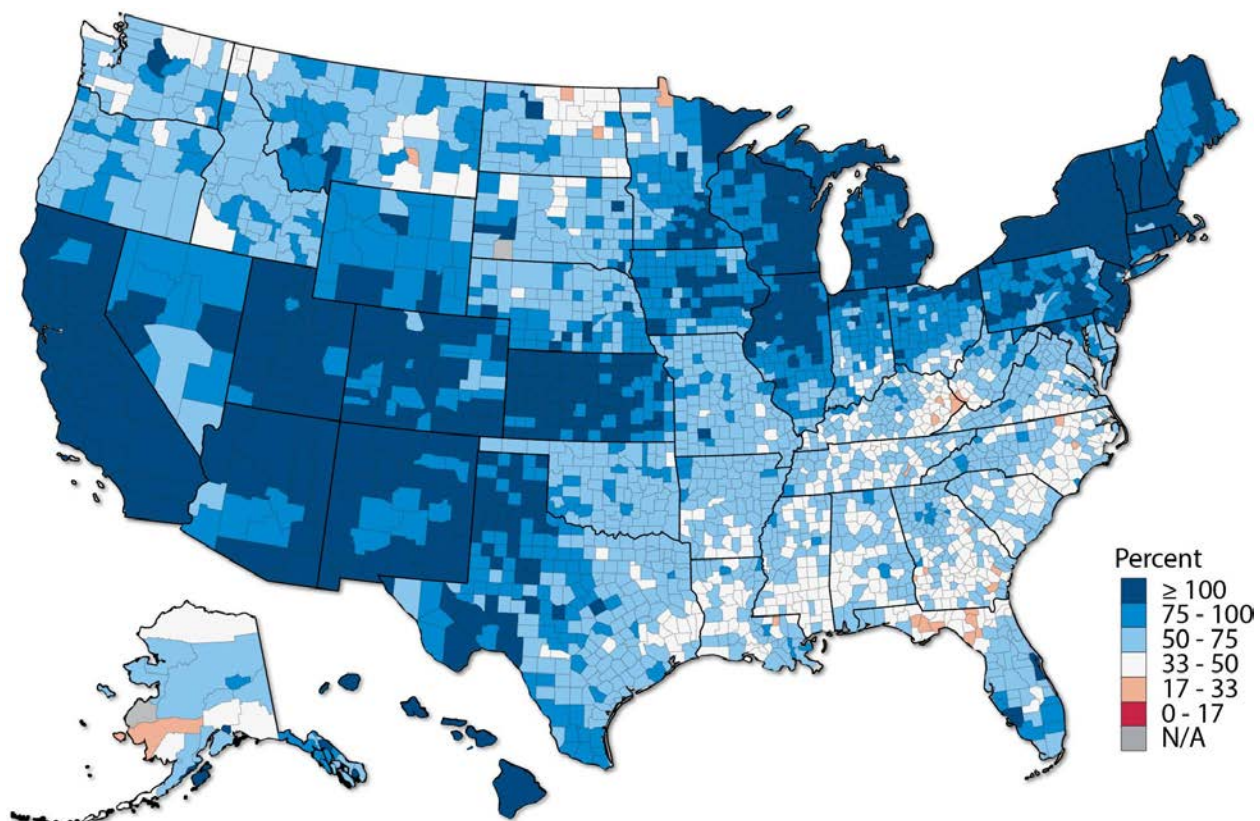
Figure 10. Percent of LMI electrical consumption that can be offset by rooftop solar generation (county)—all LMI buildings
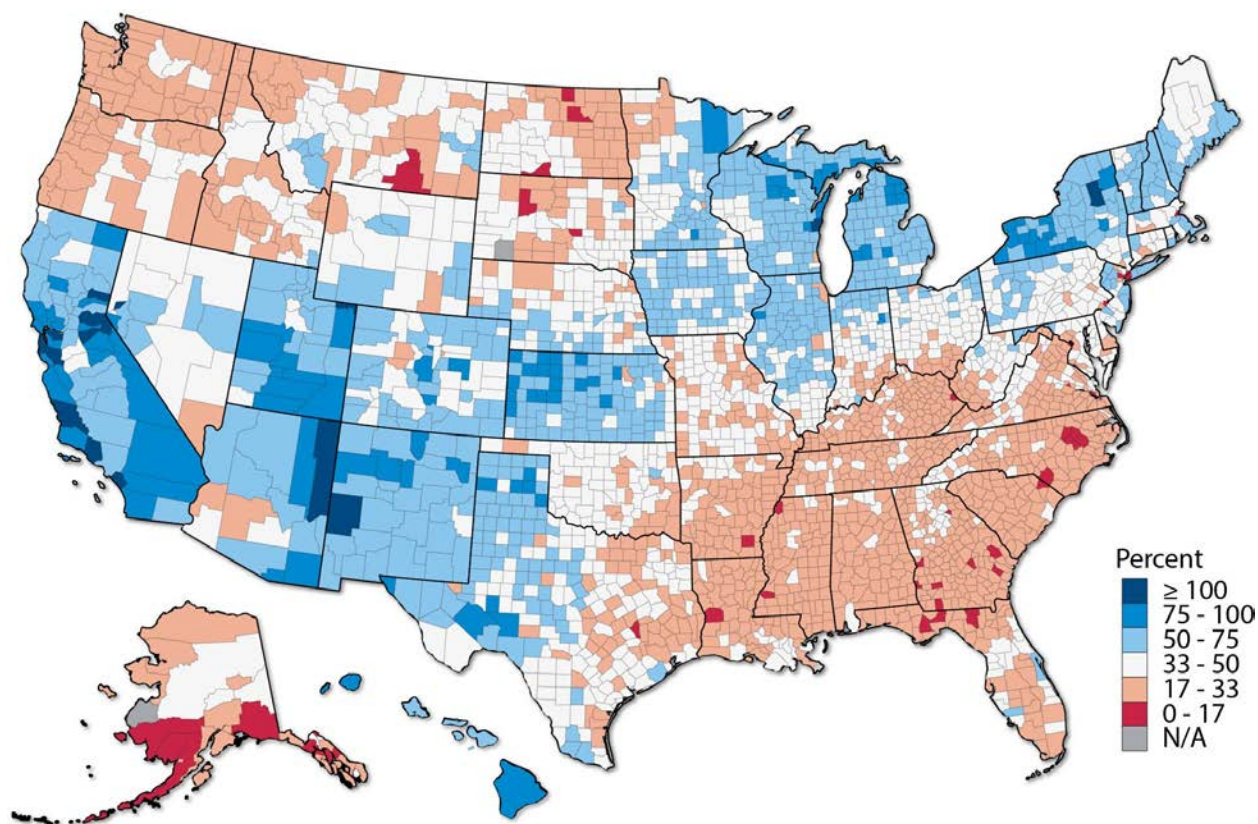
Figure 11. Percent of LMI electrical consumption that can be offset by rooftop solar generation (county)—single-family owner-occupied LMI buildings only

From a technical basis alone, there is sufficient rooftop space on LMI buildings for at least 33% of their electrical consumption to be met with rooftop solar generation. However, reaching this penetration level would require alternative deployment models than commonly found today. These models should address coordination issues inherent to rental-occupied and multi-family buildings as well as LMI financing and affordability barriers (Cook and Bird 2018). Such models should also ensure that rental property owners are incentivized to install solar on their buildings—for example, by bundling utility expenses with rent payments as a means of passing through savings to the renter. Alternatively, various shared solar models (Feldman et al. 2015), including virtual net metering, could be effective in allowing building owners to sell rooftop generation directly to their occupants. Similar issues exist for multi-family buildings, where shared solar or community solar models could help to address tenant-owner coordination issues. Some of the coordination issues, however, might be too intractable to resolve. For this reason, this report also includes penetration statistics considering only single-family owner-occupied buildings, which essentially identifies the quantity of off-site solar generation (e.g., community solar or utility-scale solar) that is needed for the penetration target.

Calculations of the potential for solar generation to offset electrical consumption are based on annual generation and consumption levels and do not consider potential mismatches at the hourly level. For many buildings, and without energy storage, these mismatches are likely to be substantial. For instance, buildings might generate more energy than consumed during midday, when irradiance is highest, resulting in excess energy exported to the grid. In contrast, during

28

periods of peak demand (e.g., afternoons and evenings), consumption could exceed generation, resulting in energy delivered from the grid. There are a few important implications of this phenomena for policymakers. One is that retail tariff design and other associated policies influence the economic value of distributed solar to LMI households, particularly, the value of excess generation exported to the grid. Without careful thought, this could limit the nominal purpose of LMI programs—energy burden reduction. Another is that these consumption and generation mismatches, sans energy storage, limit the ability for distributed solar to provide resiliency benefits, which also could be a policy goal. Finally, LMI solar should be considered more broadly in the perspective of transmission and distribution grid-integration issues, such as the energy and capacity value of solar energy, potential for solar overgeneration, and the hosting capacity of local distribution networks. For more details on some of these issues see Denholm et al. (2016) and Palmintier et al. (2016).

3.2.1. Additional Factors Impacting Building Technical Suitability

Although the LiDAR method for assessing technical potential accounts for several important factors that can affect rooftop suitability (e.g., unshaded area, tilt, azimuth), it excludes other factors that also might matter. For instance, it is generally not advised to install solar panels on older roofs, because it is costly to uninstall solar panels prior to replacing the roof. Thus, although roof age is categorized as an economic factor and not a technical factor, it impacts the building suitability and overall market potential. Other salient factors that could impact a building's suitability can include electrical code or interconnection issues, unsuitability of the roof to support the weight of the panels and racking (e.g. flat roof without enough support or a mobile home), and existing violations of building codes that are cost-prohibitive to address in the installation.

To estimate what proportion of LMI buildings might face these types of challenges, we analyzed historical data from GRID Alternatives installations, a non-profit provider of solar to low-income households. Because the data are collected primarily for single-family homes in California, the descriptive statistics are not intended to be representative of other geographies or for multi-family buildings. Nevertheless, these data provide a first-of-kind insight into the frequency of additional barriers to solar deployment. Determining the economic feasibility of preparing a roof for solar installation often requires physical inspection and is beyond the scope of this report to conclusively address.

Based on a sample of 24,269 potential solar installations ("leads"), we identified 10 reasons why a building was determined—either by physical inspection or in conversation—to be unsuitable for solar: Old roof (n = 1,474), excessive (unspecified) upgrades required (n = 552), building code issues (n = 340), roof shading (n = 314), electrical service issues (n = 187), unsafe roof pitch (n = 152), insufficient roof space (n = 137), mobile home (n = 117), roof orientation (n = 47), and roof type (n = 31). Of these 10 reasons, "roof space," "roof orientation," "roof shading," and "unsafe roof pitch" are excluded, as these factors already are considered in the LiDAR method. "Mobile home" also is excluded because these buildings already were excluded from the present technical potential analysis. Additionally, of the 24,269 leads, 10,781 were excluded for non-technical reasons (disinterest in solar n = 4,224; ineligibility to receive low-income solar grants n = 6,557) and did not receive technical evaluations, so it is undetermined whether these leads would have been technically suitable. Thus, it's estimated that 10.5% to 18.9% of low-

income buildings could face additional techno-economic barriers to solar beyond those considered in the LiDAR method alone. Readers are urged to use caution in interpreting this data due to representativeness issues. Future work should couple physical inspections with technical potential assessments.

3.3. Technical Potential for Select Buildings that Serve LMI Households

Next, we investigate the possible role for third-party buildings that serve low-income populations to host solar on their roofs. Solar deployed on these third-party buildings could either reduce operational costs, thereby helping to expand mission-related activities, or capacity could explicitly be designated to offset local electrical consumption via a virtual net metering arrangement. The specific building classes investigated are public sites (e.g., libraries, police stations, local government), public housing (i.e., federally assisted rental housing), K–12 public schools, homeless shelters, and places of worship. These building classes are not intended to be comprehensive of all third-party buildings that could deploy solar. Results for this section are presented for the three cities analyzed in greater depth in the forthcoming companion report (Chicago, Illinois; San Bernardino/Riverside, California; and Washington, D.C.). Methods for collecting the data involved manual effort (*see* Appendix D), so at this time we are unable to present a national assessment of the five building types.

To quantify the technical potential of LMI-serving buildings in the cities, we obtained GIS data for each building type and spatially tagged these layers to the LiDAR buildings database. The LMI-serving building data is an agglomerate data set from a variety of sources. Because the data consists of varied data sets and formats, multiple methods were used to tag each building geometry to one or more LiDAR building footprint. Jointly, this enabled identification of the total technical potential for each building type in each city. Appendix D provides further detail on methods and data sources.

Over the five building classes, schools have the greatest technical potential opportunity by far, although there are substantial opportunities for all the classes examined (*see* Table 8). Collectively the gross generation potential for the five building classes is estimated to be 1,012.2 GWh, 311 GWh, and 377.1 GWh for Chicago, San Bernardino/Riverside, and Washington, D.C. respectively. These generation estimates are based on the solar suitability criteria (i.e., non-North facing) and do not include the possible on-site area available for ground-mounted systems. To put these values in context, they represent approximately 13%, 29%, and 9% of the estimated annual electricity consumption of low- to moderate-income households in the city.

30

Table 9. Annual Generation Potential for Select Third-Party Buildings in Chicago, Washington D.C., and San Bernardino/Riverside (GWh)

	Chicago	San Bernardino/ Riverside	Washington, D.C.
Public Housing	62.8	16.6	31.0
Public Sites	51.9	24.422	41.1
K–12 Schools	306.4	106.2	73.0
Homeless Shelters	5.3	0.6	5.6
Places of Worship	108.1	7.3	32.8
Total (GWh)	1072.3	311.0	377.1

Next, on-site electrical consumption of each of the third-party buildings is estimated to determine the feasibility of oversizing a PV system with the purpose of using excess solar generation to offset nearby LMI households. To estimate the on-site consumption, each building was matched with a comparable representative building in the EIA Residential and Commercial Building Energy Consumption Surveys and—to match local climate-related consumption patterns—to the nearest Census Division (EIA 2013; EIA 2016a). This allows us to derive the average electrical consumption per square foot of building footprint for each building type, which then is multiplied by the building footprint of each of the third-party buildings in the LiDAR database. When sizing the PV system for each building the same suitability criteria is used (e.g., no installation on north-facing roof planes), and it is assumed that each building offsets 100% of its on-site consumption before exporting generation to the community. Finally, this method only considers generation and consumption on an annual basis and does not consider potential mismatches in the hourly profiles. Appendix D describes this process in more detail.

We find that, after accounting for on-site consumption, the five third-party building types considered could feasibly oversize PV systems on their roofs such that excess generation accounts for 1.3% to 8.7% of LMI consumption in the city (Table 9), and the opportunity differed substantially between cities. Due to the greatest solar resource of the three regions, San Bernardino/Riverside had the highest generation excess fraction, and it is estimated that third-party buildings' excess could account for 8.7% of LMI consumption. For Washington, D.C.—the smallest fraction—it is estimated third-party buildings excess could account for 1.3% of LMI consumption.

Schools, followed by Places of Worship were consistently the highest opportunity of the five building classes considered. Both buildings typically are in residential neighborhoods. Schools usually have large flat roofs and low consumption in the summer, when solar irradiance is highest. Places of Worship had low levels of electricity consumption and moderately favorable roof characteristics. The results also indicate that Public Housing, Public Sites, and Homeless Shelters likely have insufficient rooftop space to offset 100% of their own on-site consumption—though actual values could vary for individual buildings.

---

[22] Due to data limitations, generation potential for San Bernardino public sites was not estimated.

Table 10. Net Excess Rooftop Potential Accounting for Building Self-Consumption by Building Class and City

	Chicago	San Bernardino/ Riverside	Washington, D.C.
Public Housing (GWh)	0.0	0.0	0.0
Public Sites (GWh)	0.0	0.0	0.0
K-12 Schools (GWh)	19.8	19.6	5.5
Homeless Shelters (GWh)	0.0	0.0	0.0
Places of Worship (GWh)	31.5	3.2	4.6
Total (GWh)	51.4	22.8	10.1
Total (% of LMI Consumption in City)	2.1%	8.7%	1.3%

4. Conclusion

This report presents a first-of-kind assessment of the technical potential of rooftop solar for low- and moderate-income households and provides insight on the distribution of solar potential by tenure, income, and other building characteristics. The research indicates that a substantial fraction (42%) of the national residential rooftop solar potential is located on LMI buildings and, for all incomes, a substantial fraction is located on multi-family and renter-occupied buildings.

We also find that rooftop solar can significantly contribute to meeting U.S. electricity demand. Specifically, from a technical basis there is sufficient rooftop space to ensure that at least 33% of U.S. residential electrical consumption is offset by rooftop solar—although to do so requires deployment on multi-family and renter-occupied buildings. Reaching this level of offset is most feasible in Northeast and Southwest portions of the United States, where per-capita electricity use is lowest. This report also highlights the importance of ensuring solar access for mobile home residents, who are disproportionately low-income yet typically cannot install rooftop solar because of structural concerns.

In cases where LMI households are unable to adopt solar for their own homes, non-profit entities might enter agreements to host solar on their own roofs. This study investigated the feasibility for five classes of buildings in Chicago, San Bernardino/Riverside, and Washington, D.C., finding that the buildings likely could oversize PV systems on their roofs equivalent to offsetting 1.3% to 8.7% of local LMI consumption. This fraction is significant but is unlikely to be a leading mechanism for increasing LMI access to solar. Future research could explore the feasibility of ground-mounted systems at strategic locations (i.e., community solar) or installation on for-profit buildings.

Traditional deployment models have insufficiently enabled access to solar for low- and moderate-income households. In part, this is because there are significant economic and financial barriers to LMI solar adoption without policy action. These include poor access to credit, low capital availability, housing uncertainty, and many more. Without innovation either in regulatory, market, or policy factors, a large fraction of the U.S. potential is unlikely to be met. Potential electric bill savings from rooftop solar would have the greatest material impact on the lives of low-income households as compared to their high-income counterparts and could help mitigate the energy burden faced by these households.

4.1. Data for Public Use

This report ultimately seeks to provide objective data for regulators, policymakers, nonprofits, and project developers to make informed decisions that are best for their own communities, for example to assess the potential for rooftop solar in their jurisdictions and perform policy cost-benefit analysis. To this effect, data used in this report is provided freely via NREL's website in two formats. One format is an interactive web application using NREL's OpenCarto platform, and was developed to enable user to browse, visualize, and export results (https://maps.nrel.gov/solar-for-all). Secondly, the technical potential data used in this report, accompanied by several additional techno-economic variables, and aggregated at the tract-level, is available for download at (https://data.nrel.gov/submissions/81). The Rooftop Energy Potential of Low Income Communities in America (REPLICA) data set includes measures of electricity

33

expenditures ($/month), demographics, utility electric rates, and other important variables compiled from a variety of sources and tagged to each Census tract.

4.2. Future Work

Three topics for future research are suggested to extend and improve this work. First, this work uses limited building-level attributes within the analysis, except for rooftop planes obtained via LiDAR. Many local governments, however, increasingly make building-level GIS files available for free or for a modest fee (i.e., tax rolls). Building-level models would permit substantially more-nuanced assessments of the technical, economic, market, and behavioral aspects of rooftop solar deployment.

Future research also could improve the representation of low-income energy consumption, perhaps also at the building level. This analysis does not identify building-level variation in consumption, which is significant. We also acknowledge our limitation in not considering hourly mismatches between consumption and solar generation, which can be significant. These mismatches—and the value of excess generation exported to the electric grid—are an important dimension of the economic evaluation.

Finally, although this analysis does identify differences in technical potential between single-family and multi-family buildings, there is room for improvement. Specifically, future research could use building-level data sets to more precisely identify the locations of multi-family low-income buildings. Future work also could improve the representation of tenant-level electrical loads versus communal building loads, as well as publish additional data distinguishing how income affects electricity consumption patterns.

References

ABB Energy. 2017. *Velocity Suite*. Data Product. Boulder, CO: ABB Energy.

Borenstein, S. 2017. "Private Net Benefits of Residential Solar PV: The Role of Electricity Tariffs, Tax Incentives, and Rebates." *Journal of the Association of Environmental and Resource Economists 4*(S1), S85–S122.

California Public Utility Commission (CPUC). 2017a. *CARE/FERA Programs.* http://www.cpuc.ca.gov/General.aspx?id=976.

California Public Utility Commission (CPUC). 2017b. "Implementation of AB 693—Solar on Multifamily Affordable Housing (SOMAH)." D.17-12-022. Accessed March 5, 2018. http://www.cpuc.ca.gov/General.aspx?id=6442454736.

Chaudhari, Maya, Lisa Frantzis, and Tom E. Hoff. 2004. *PV Grid Connected Market Potential Under a Cost Breakthrough Scenario.* Chicago: Navigant Consulting. 2004-117373.

Cole, W., B. Frew, P. Gagnon, J. Richards, Y. Sun, J. Zuboy, M. Woodhouse, R. Margolis. 2017. *SunShot 2030 for Photovoltaics (PV): Envisioning a Low-Cost PV Future*. Golden, CO: National Renewable Energy Laboratory. NREL/TP-6A20-68105.

Cook, J., and L. Bird. 2018. *Unlocking Solar for Low- and Moderate-Income Residents: A Matrix of Financing Options by Resident, Provider, and Housing Type*. Golden, CO: National Renewable Energy Laboratory. NREL/TP-6A20-70477.

Denholm, Paul, Kara Clark, and Matt O'Connell. 2016. *On the Path to SunShot: Emerging Issues and Challenges in Integrating High Levels of Solar into the Electrical Generation and Transmission System.* Golden, CO: National Renewable Energy Laboratory. NREL/TP-6A20-65800. http://www.nrel.gov/docs/fy16osti/65800.pdf.

Denholm, Paul, and Robert Margolis. 2008. *Supply Curves for Rooftop Solar PV-Generated Electricity for the United States.* Golden, CO: National Renewable Energy Laboratory. NREL/TP-6A20-44073.

DOE Better Buildings (2017, December 5). *Denver Housing Authority Launches Community Solar Garden*. https://betterbuildingsinitiative.energy.gov/beat-blog/denver-housing-authority-launches-community-solar-garden (accessed March 19, 2018).

Federal Emergency Management Agency (FEMA). 2016. Summary of Databases in Hazus-Multi Hazard. http://www.fema.gov/summary-databases-hazus-multi-hazard (accessed March 4, 2016).

Feldman, D., A. Brockway, E. Ulrich, and R. Margolis. 2015. *Shared Solar: Current Landscape, Market Potential, and the Impact of Federal Securities Regulation.* NREL/TP-6A20-63892.

Gagnon, Pieter, Robert Margolis, Jennifer Melius, Caleb Phillips, and Ryan Elmore. 2016. *Rooftop Solar Photovoltaic Technical Potential in the United States: A Detailed Assessment*. NREL/TP-6A20-65298.

Gagnon, P., R. Margolis, J. Melius, C. Phillips, and R. Elmore. 2018. "Estimating Rooftop Solar Technical Potential Across the US Using a Combination of GIS-Based Methods, LiDAR Data, and Statistical Modeling." Environmental Research Letters.

GTM Research. 2017. Q4 2017, U.S. Solar Market Insight.

Lopez, A.; B. Roberts, D. Heimiller, N. Blair, and G. Porro. 2012. *U.S. Renewable Energy Technical Potentials: A GIS-Based Analysis*. National Renewable Energy Laboratory (NREL), Golden, CO. Golden, CO: National Renewable Energy Laboratory. NREL/TP-6A20-51946.

Manson, S., J. Schroeder, D. Van Riper, and S. Ruggles. 2017. IPUMS National Historical Geographic Information System: Version 12.0 [Database]. Minneapolis: University of Minnesota. http://doi.org/10.18128/D050.V12.0c.

Margolis, R., P. Gagnon, J. Melius, C. Phillips, and R. Elmore. 2017. "Using GIS-Based Methods and LiDAR Data to Estimate Rooftop Solar Technical Potential in U.S. Cities." *Environmental Research Letters* 12(7), 074013.

Moezzi, M., A. Ingle, L. Lutzenhiser, and B. Sigrin. 2017. *A Non-Modeling Exploration of Residential Solar Photovoltaic (PV) Adoption and Non-Adoption.* National Renewable Energy Laboratory (NREL). Golden, CO: National Renewable Energy Laboratory. NREL/SR-6A20-67727.

Multi-Resolution Land Characteristics Consortium (MRLC). 2011. "National Land Cover Database 2011." https://www.mrlc.gov/nlcd11_data.php (accessed December 15, 2017).

National Renewable Energy Laboratory (NREL). December 15, 2017. *NREL's PVWatts Calculator*. http://pvwatts.nrel.gov/ (accessed March 18, 2018).

Olsson, Ulf. 2005. "Confidence Intervals for the Mean of a Log-Normal Distribution." *Journal of Statistics Education* 13(1).

Paidipati, J., L. Frantzis, H. Sawyer, and A. Kurrasch. 2008. *Rooftop Photovoltaics Market Penetration Scenarios*. Golden, CO: National Renewable Energy Laboratory (work performed by Navigant Consulting). NREL/SR-581-42306.

Palmintier, Bryan, Robert Broderick, Barry Mather, Michael Coddington, Kyri Baker, Fei Ding, Matthew Reno, Matthew Lave, and Ashwini Bharatkumar. 2016. *On the Path to SunShot: Emerging Issues and Challenges in Integrating Solar with the Distribution System*. Golden, CO: National Renewable Energy Laboratory. NREL/TP-5D00-65331. http://www.nrel.gov/docs/fy16osti/65331.pdf.

Phillips, Caleb, and Jenny Melius (2016). *U.S. PV-Suitable Rooftop Resources. National Renewable Energy Laboratory*. https://dx.doi.org/10.7799/1258436.

Rosenblatt, Murray. 1956. "Remarks on Some Nonparametric Estimates of a Density Function." Annals of Mathematical Statistics. 27, no. 3, 832-837.

U.S. Census Bureau. 2010. "Geographic Terms and Concepts—Census Divisions and Census Regions." *2010 Census*. https://www2.census.gov/geo/docs/maps-data/maps/reg_div.txt.

U.S. Census Bureau. 2015a. "B19001: Household Income in the Past 12 Months (in 2015 Inflation-Adjusted Dollars)." *2011–2015 American Community Survey*. Retrieved from website https://www.nhgis.org/.

U.S. Census Bureau. 2015b. "B25118: Tenure by Household Income in the Past 12 Months (in 2015 Inflation-Adjusted Dollars)." *2011–2015 American Community Survey*. https://www.nhgis.org/ (accessed April 17, 2017).

U.S. Census Bureau. 2015c. "B25124: Tenure by Household Size by Units in Structure." *2011–2015 American Community Survey*. https://www.nhgis.org/ (accessed April 17, 2017).

U.S. Census Bureau. 2015d. "B25032: Tenure by Units in Structure." *2011–2015 American Community Survey*. https://www.nhgis.org/ (accessed April 17, 2017).

U.S. Department of Energy (DOE), Weatherization and Intergovernmental Office. *Weatherization Assistance Program*. https://www.energy.gov/eere/wipo/weatherization-assistance-program (accessed March 18, 2018).

U.S. Department of Energy's Office of Energy Efficiency and Renewable Energy (DOE EERE). 2017. "Low-Income Energy Affordability Data (LEAD) Tool." https://catalog.data.gov/dataset/clean-energy-for-low-income-communities-accelerator-energy-data-profiles-2fffb (accessed December 15, 2017).

U.S. Department of Housing and Urban Development (HUD). 2016. "Income Limits." https://www.huduser.gov/portal/datasets/il.html#2016 (accessed March 19, 2018).

U.S. Department of Housing and Urban Development's Office of Policy and Developed & Research (HUD PD&R). 2016. "HUD Income Limits Briefing Material." https://www.huduser.gov/portal/datasets/il//il16/IncomeLimitsBriefingMaterial-FY16.pdf (accessed December 15, 2017).

U.S. Energy Information Administration (EIA). 2013. "2009 Residential Energy Consumption Survey (RECS)." http://www.eia.gov/consumption/residential/data/2009/index.cfm?view=microdata (accessed December 15, 2017).

U.S. Energy Information Administration (EIA). 2016a. "2012 Commercial Building Energy Consumption Survey (CBECS) Public Use Microdata." https://www.eia.gov/consumption/commercial/data/2012/index.php?view=microdata (accessed December 15, 2017).

U.S. Energy Information Administration (EIA). 2016b. "Detailed State Data: Average Price by State by Provider (EIA-861) Public Use Microdata." http://www.eia.gov/electricity/data/eia861/ (accessed December 15, 2017).

U.S. Energy Information Administration (EIA). 2017. "What is U.S. electricity generation by energy source?" https://www.eia.gov/tools/faqs/faq.php?id=427&t=3%22 (accessed March 7, 2018).

U.S. Health and Human Services (HHS). 2017. "About LIHEAP." https://www.acf.hhs.gov/ocs/programs/liheap/about (accessed December 15, 2017).

U.S. National Center for Education Statistics (NCES). 2015. "Locale Boundaries." *Education Demographic and Geographic Estimates (EDGE)*. https://nces.ed.gov/programs/edge/geographicLocale.aspx (accessed October 1, 2017).

Vaishnav, P.; N. Horner, and I. Azevedo, 2017. "Was It Worthwhile? Where Have the Benefits of Rooftop Solar Photovoltaic Generation Exceeded the Cost?" *Environmental Research Letters* 12(9).

Wilcox, S., and W. Marion. 2008. *User's Manual for TMY3 Data Sets*. Golden, CO: National Renewable Energy Laboratory. NREL/TP-581-43156.

Appendix A. Allocation of Demographic Attributes

This appendix describes the series of data transformation steps used to identify cross-tabulations (i.e., "crosstabs") of demographic attributes at the Census tract level by income, building type, and tenure. This process relies on a set of tables (Table 3) from the 2011–2015 5-year American Community Survey (ACS). In general, we rely on four major steps when generating a tract-level crosstab of household counts by income, building type, and tenure, namely:

1. Calculate the number of households belonging to each $1,000 income group, at the tract level.

2. Disaggregate from county data to estimate the number of households, per $1,000 income group, per tenure, at the tract level.

3. Disaggregate from county data to estimate the number of households, per $1,000 income group, per tenure, per dwelling type, per household size.

4. Aggregate tract estimates by AMI income group. Create final data set of number of households by AMI income group, by building type, and by tenure, per tract.

Each of these steps involves a series of data transformations and relies on a set of statistical sampling assumptions. Described below are these methods and assumptions for each step in more detail.

A.1. Calculate the Number of Households Belonging to Each $1,000 Income Group, at the Tract Level

In the first step of the ACS data processing methodology, we use the tract level "*Household Income in the Past 12 Months (in 2015 Inflation-Adjusted Dollars)*" ACS table, which provides tract-level household counts classified according to ACS income bins.[23] We take this table and deconstruct the ACS predefined income brackets into $1,000 increments. To do so, we randomly sample $1,000 increments for each bin assuming that income is uniformly distributed within the bin. We also assign a maximum income cap of $1,000,000/year because no identification in our results is needed at this resolution.

Disaggregating these ACS defined income bins into $1,000 increments serves two purposes. First, it allows us to reconcile ACS tables with different income binning (e.g. $35,000–$39,000 versus $35,000–$49,000 reported in the county data set). Second, it allows us to more precisely allocate incomes to different AMI income groups.

---

[23] ACS tract-level incomes are classified into 14 bins, namely: $0–$10,000, $10,000–$14,000, $15,000–$19,000, $20,000–$24,000, $25,000–$29,000, $30,000–$34,000, $35,000–$39,000, $40,000–$44,000, $45,000–$49,000, $50,000–$59,000, $60,000–$74,000, $75,000–$99,000, $100,000–$124,000, $125,000–$149,000, $150,000–$199,000, and $200,000 or more.

A.2. Disaggregate from County Data to Estimate the Number of Households, per $1,000 Income Group, per Tenure, at the Tract Level

Next, we disaggregate county demographic crosstabs to the tract level, using the tract household counts as the disaggregating factor. We start with the "Tenure by Household Income in the Past 12 Months (in 2015 Inflation-Adjusted Dollars)" ACS table at the county level. To disaggregate this county data to get the estimates at the tract level, we rely on a random-weighted sampling method, weighted by the total household counts per income bin. Because we do not have the desired income by tenure data at the tract level, we rely on these random-weighted methods to help us disaggregate. In doing so, we do not directly assume that the county-to-tract counts are proportional. Rather, we assume that there is some variability across the component tracts, but this variability is inevitably weighted by tract household counts per income. This approach allows us to obtain tract-level estimates of the number of households, per $1,000 income group, per tenure.

A.3. Disaggregate from County Data to Estimate the Number of Households, per $1,000 Income Group, per Tenure, per Dwelling Type, per Household Size

This next process is similar to that described in A.2 above. Here we rely on two ACS county-level tables, namely, "*Tenure by Units in Structure*" and "*Tenure by Household Size by Units in Structure.*" We first combine these two tables using a proportional allocation method, joining based on the shared tenure field. Doing so gives us a county cross-tabulation of tenure, by units in structure, by household size. We use this county crosstab to then disaggregate to the tract level. Using the data set created in the previous step (A.2), we use a random-weighted sampling methodology to disaggregate the county crosstab. Similar to A.2, we do not assume that the county-to-tract disaggregation is directly proportional to the total household counts. Instead, we know there is variability across tract components, therefore, we use the random-weighted methodology to allow for variation, but ultimately, weighted by total counts.

A.4. Aggregate Tract Estimates by AMI Income Group

Using this large tract-level crosstab described above (Section A.1 though Section A.3), we assign the AMI income group break limits to classify the data according to our five AMI income groups: Very Low Income (0% to 30% AMI), Low Income (30% to 50% AMI), Moderate Income (50% to 80% AMI), Middle Income (80% to 120% AMI), and High Income (>120% AMI). To do so, we join the "*2016 HUD Income Limits*" (HUD 2016) table to each row in our data set based on the Census Tract location, household size, and the $1,000-increment binned yearly household income. With the data categorized into our five income groups, we remove the household size category and aggregate the final data set by the income group, building type, and tenure.

This report is available at no cost from the National Renewable Energy Laboratory (NREL) at www.nrel.gov/publications.

Appendix B. Validation of Monte Carlo Simulations for Building Sampling

This analysis uses a stochastic process to sample residential buildings in LiDAR covered Census Tracts (Section 2.3.2) to derive tract-level estimates. As such, we rely on a Monte-Carlo methodology to generate probability distributions of tract-level technical potential, per building type. The workflow is run 100 times, each using a different random seed, and the median value over the 100 runs is used as the final estimate to obtain a more accurate estimate of the technical potential in each tract.

To validate our sampling methodology and better understand the variability of the technical potential estimates, we calculate the coefficients of variance across Monte Carlo runs for tracts and cities; city coefficients of variance are detailed in Table B-1. For each run, we calculate the tract and city technical potential averages. Doing so, we find that both the average tract and city errors are low, 6.8% and 1.1% for tracts and cities, respectively. When plotting these error ratios at the tract level (Figure B-1), we find that the distribution is lognormally distributed, indicating most tracts have relatively high levels of certainty (low levels of variability) across sampled runs. The low coefficient of variance helps to validate the results and give confidence that the sampling methodology estimates technical potential of residential buildings per tract and building type with minimal error.
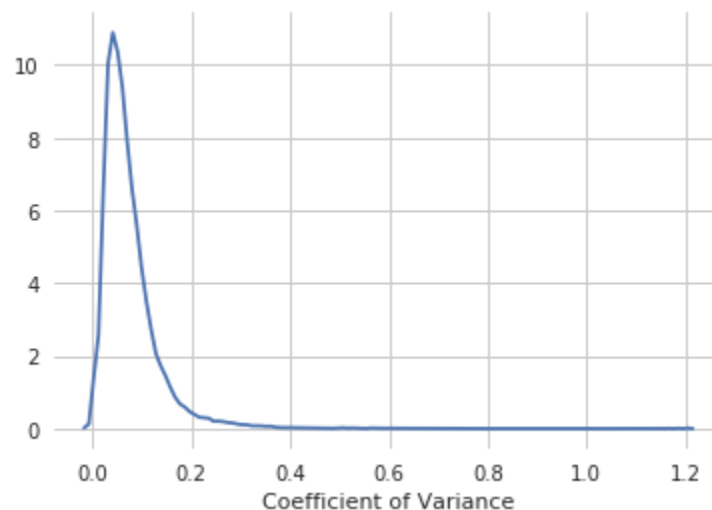
Figure B-1. Density function of coefficient of variance in the tract-level technical potential, for all tracts with LiDAR coverage[24]

---

[24] This graph plots the distribution of the coefficient of variance of technical potential for each tract with LiDAR coverage. Each point in the plot represents the coefficient of variance for a single tract across the 100 runs. The data is graphed using a Kernel Density Estimation (KDE) plot, a non-parametric technique to estimate the probability density function and visualize the underlying distribution of a continuous variable (Rosenblatt 1956). Notably, because of smoothing used by the plotting library, the x-axis is not constrained to the minimum 0 bound.

Table B-1 demonstrates the mean technical potential over the 100 Monte Carlo runs for each city with LiDAR coverage and the standard deviation. Notably, there is more uncertainty in smaller cities (e.g., Frankfort, KY) with fewer Census Tracts than the larger metropolitan cities (e.g., New York, NY). This result is intuitive because model error is the greatest at the tract level and reduced when tract-level estimates are aggregated over larger areas.

Table B-1. Assumptions for PV Performance Simulations Summary Statistics for City-Level Technical Potential[25]

LiDAR City	LiDAR State	Mean (GWh)	STD (GWh)	Coefficient of Variance
Albany	NY	1.9	0.015	0.008
Albuquerque	NM	3.2	0.022	0.007
Allentown	PA	2.0	0.018	0.009
Amarillo	TX	2.2	0.025	0.012
Anaheim	CA	3.9	0.060	0.015
Atlanta	GA	1.0	0.029	0.028
Augusta	GA	2.7	0.029	0.011
Augusta	ME	1.8	0.078	0.043
Austin	TX	2.2	0.024	0.011
Bakersfield	CA	3.0	0.014	0.005
Baltimore	MD	1.4	0.009	0.007
Baton Rouge	LA	3.7	0.040	0.011
Birmingham	AL	1.6	0.029	0.017
Bismarck	ND	2.3	0.036	0.016
Boise	ID	3.3	0.025	0.008
Boulder	CO	1.8	0.032	0.018
Bridgeport	CT	1.8	0.023	0.013
Buffalo	NY	2.0	0.013	0.007
Carson City	NV	2.3	0.091	0.039
Charleston	SC	1.5	0.024	0.016
Charleston	WV	1.9	0.022	0.012
Charlotte	NC	2.4	0.026	0.011
Cheyenne	WY	2.3	0.040	0.018
Chicago	IL	1.3	0.006	0.004

---

[25] The LiDAR cities listed in Table B-1 do not necessarily align with the legal footprints of city or metropolitan area boundaries. Rather they refer to the focal city covered in the LiDAR raster extent. A single LiDAR city extent can span multiple cities and states (e.g. Washington D.C. covers much of Northern Virginia and southern Maryland cities in addition to the District of Columbia) or they can only span partial cities (e.g. Richmond, VA, is only 55% covered by its LiDAR raster extent).

LiDAR City	LiDAR State	Mean (GWh)	STD (GWh)	Coefficient of Variance
Cincinnati	OH	1.5	0.011	0.008
Cleveland	OH	1.2	0.008	0.006
Colorado Springs	CO	2.5	0.014	0.006
Columbia	SC	2.2	0.031	0.014
Columbus	GA	2.7	0.031	0.011
Columbus	OH	2.2	0.016	0.007
Concord	NH	1.8	0.070	0.039
Corpus Christi	TX	2.4	0.052	0.022
Dayton	OH	2.2	0.019	0.009
Denver	CO	2.0	0.010	0.005
Des Moines	IA	2.2	0.031	0.014
Detroit	MI	1.2	0.007	0.006
Dover	DE	2.6	0.075	0.029
El Paso	TX	3.4	0.028	0.008
Flint	MI	2.1	0.019	0.009
Fort Wayne	IN	1.6	0.027	0.017
Frankfort	KY	3.0	0.083	0.028
Fresno	CA	2.4	0.014	0.006
Fort Belvoir	DC	1.7	0.044	0.026
Grand Rapids	MI	3.8	0.051	0.013
Greensboro	NC	2.4	0.025	0.011
Harrisburg	PA	2.9	0.023	0.008
Hartford	CT	1.6	0.014	0.009
Helena	MT	2.2	0.045	0.020
Houston	TX	3.0	0.017	0.006
Huntsville	AL	3.9	0.026	0.007
Indianapolis	IN	2.6	0.018	0.007
Jackson	MS	1.9	0.024	0.013
Jacksonville	FL	2.5	0.026	0.011
Jefferson City	MO	4.2	0.106	0.025
Kansas City	MO	1.7	0.012	0.007
Lancaster	PA	2.9	0.038	0.013
Lansing	MI	2.3	0.036	0.016
Las Vegas	NV	1.8	0.011	0.006
Lexington	KY	2.5	0.024	0.010

LiDAR City	LiDAR State	Mean (GWh)	STD (GWh)	Coefficient of Variance
Lincoln	NE	1.8	0.022	0.012
Little Rock	AR	2.0	0.026	0.013
Los Angeles	CA	2.3	0.007	0.003
Louisville	KY	1.8	0.045	0.025
Lubbock	TX	2.8	0.030	0.011
Madison	WI	2.2	0.022	0.010
McAllen	TX	5.6	0.038	0.007
Miami	FL	3.1	0.009	0.003
Milwaukee	WI	1.7	0.013	0.008
Minneapolis	MN	1.7	0.011	0.007
Mission Viejo	CA	3.5	0.024	0.007
Mobile	AL	1.1	0.021	0.019
Modesto	CA	3.0	0.037	0.013
Montgomery	AL	3.0	0.037	0.012
Montpelier	VT	1.8	0.058	0.032
New Haven	CT	2.1	0.021	0.010
New Orleans	LA	2.3	0.008	0.004
New York	NY	0.7	0.003	0.004
Norfolk	VA	2.0	0.010	0.005
Oklahoma City	OK	2.7	0.014	0.005
Olympia	WA	3.1	0.032	0.010
Omaha	NE	2.1	0.013	0.006
Orlando	FL	3.2	0.032	0.010
Oxnard	CA	3.4	0.028	0.008
Palm Bay	FL	5.9	0.029	0.005
Pensacola	FL	3.4	0.037	0.011
Philadelphia	PA	1.6	0.007	0.004
Pittsburgh	PA	1.3	0.008	0.006
Portland	OR	2.1	0.011	0.005
Poughkeepsie	NY	2.0	0.016	0.008
Providence	RI	1.6	0.014	0.009
Raleigh-Durham	NC	1.9	0.019	0.010
Reno	NV	2.0	0.027	0.013
Richmond	VA	0.8	0.019	0.024
Rochester	NY	1.4	0.019	0.013

LiDAR City	LiDAR State	Mean (GWh)	STD (GWh)	Coefficient of Variance
Sacramento	CA	2.2	0.013	0.006
Salem	OR	3.1	0.029	0.009
Salt Lake City	UT	2.1	0.018	0.009
San Antonio	TX	3.4	0.014	0.004
San Bernardino–Riverside	CA	2.9	0.016	0.006
San Diego	CA	2.1	0.013	0.006
San Francisco	CA	2.5	0.009	0.004
Santa Fe	NM	3.2	0.043	0.013
Sarasota	FL	7.3	0.039	0.005
Scranton	PA	1.4	0.018	0.013
Seattle	WA	1.5	0.012	0.008
Shreveport	LA	2.6	0.028	0.011
Spokane	WA	1.5	0.014	0.010
Springfield	IL	2.1	0.023	0.011
Springfield	MA	1.1	0.018	0.016
St Louis	MO	2.4	0.011	0.005
Stockton	CA	2.4	0.026	0.011
Syracuse	NY	1.4	0.021	0.015
Tallahassee	FL	2.2	0.032	0.015
Tampa	FL	2.4	0.023	0.010
Toledo	OH	1.0	0.014	0.014
Topeka	KS	2.3	0.028	0.012
Trenton	NJ	1.5	0.027	0.018
Tucson	AZ	3.2	0.022	0.007
Tulsa	OK	2.7	0.020	0.007
Washington	DC	1.7	0.006	0.003
Wichita	KS	1.9	0.020	0.011
Winston-Salem	NC	2.2	0.030	0.014
Worcester	MA	1.5	0.021	0.014
Youngstown	OH	2.2	0.024	0.011

Appendix C. Predictive Modeling Framework for Imputing Solar Suitability

This appendix describes the predictive modeling framework used in this analysis to impute solar suitability for the 63% of Census Tracts without LiDAR coverage. The overall framework builds off the original methodology developed by Gagnon et al. (2016) to impute solar suitability for small, medium, and large buildings in zip codes without LiDAR data. The approach here extends this work by increasing the spatial fidelity of the statistical model used for imputation (i.e., tracts versus zip codes) and adding an additional submodel to aid in predicting suitability across residential building types, per income, building type, and tenure. In total, there are four submodels used for the imputation.

1. Household-to-Building Model
2. Small Building Suitability Model
3. Rooftop Tilt and Azimuth Model
4. Rooftop Plane Area Model

The following sections explore each submodel in greater detail.

C.1. Household-to-Building Model

The household-to-building model is a composite model that estimates the number and size of buildings (i.e., small, medium, large) for each tract outside of the LiDAR covered extents. The model is comprised of two submodels: (1) the household-to-building-count model, and (2) the building-type-to-building-size model. Both submodels rely on a distribution sampling approach for imputing values from simulated LiDAR estimates.

C.1.1. Household-to-Building-Count Ratios

The household-to-building-count submodel uses the ACS-derived tract-level crosstab of household counts to estimate number of buildings per building type for an imputed tract based on the number of households in the tract. Ratio distributions are created for multi-family buildings only. For single-family buildings, we assume a one-to-one ratio of number of households to number of buildings. This study does not account for vacant or seasonal housing. For multi-family buildings, we calculate the mean household-to-building-count ratio for 2–4-unit, 5–19 unit, and 20+ unit multi-family buildings in LiDAR covered Census Tracts. These mean ratios (Table C-1) are used to impute tracts outside of the LiDAR coverage and translate household counts to building counts.

Table C-1. National Mean Household-to-Building Ratio

Building Type	Ratio
Multi-Family 2–4 Units	3.28
Multi-Family 5–19 Units	9.14
Multi-Family 20+ Units	80.0

C.1.2. Building-Type-to-Building-Size Ratios

The building-type-to-building-size submodel translates the building counts from Table C-1 into counts by building size (e.g. small, medium, large). Categorizing building counts by size aligns our data set for national imputation using the methods developed by Gagnon et al. (2016). Like that shown above, this model is performed on multi-family buildings only; for single-family detached, we assume all buildings are small. For multi-family buildings, we compute national means of the smallest size ratios for each multi-family building type and use these to sample sizes in Census Tracts without LiDAR data. For 2–4 unit and 5–19-unit multi-family buildings, we take the mean of the percent of the buildings that are small (compared to those that are medium sized), and for 20+ unit buildings, we take the mean of the percent that are medium (compared to those that are large sized). These national averages of building size ratios per building type are depicted in Table C-2.

Table C-2. National Mean Building Type to Building Size Ratio for Census Tracts

Building Type	Ratio Type	Ratio
Multi-Family 2 to 4 Units	Small to Medium	68%
Multi-Family 5 to 19 Units	Small to Medium	60%
Multi-Family 20+ Units	Medium to Large	73%

C.2. Small Building Suitability Model

Gagnon et al. (2016) found that medium and large buildings are almost unanimously suitable, because they are overwhelmingly flat with at least one $10m^2$ plane, and small buildings ($<=5{,}000$ ft^2) suitability was more variable. For these reasons, we apply a predictive modeling approach for estimating small buildings' suitability. For medium and large buildings, we assume a percent suitability of 100%. The following describes the small building suitability model.

The small building suitability model is a multiple regression model for describing percent suitability of small buildings (Gagnon et al. 2016). It relies on data from the U.S. National Land Cover Database (NLCD) (MRLC 2011), the National Center for Education Statistics (NCES 2015), and the U.S. Census Bureau (U.S. Census 2010). Predictive variables include the northing, locale, census division, and percent land cover for water, developed open space, developed high-intensity, and all forest-type land uses. The model specification is shown in (1).

$$\text{Percent\_Suitable} = \text{Locale}*\text{Census\_Region} + \text{Northing} + \text{Water} + \text{Forest} + \text{Developed\_Open\_Space} + \text{Developed\_High\_Intensity} \tag{1}$$

Though the model originally was applied to zip codes, it was designed to be applied using any geographic area. This analysis utilizes this model and applies it to the Census Tract. As such, we used tract-specific data (e.g., assigning the locale of a tract based on the tract centroid rather than the centroid of the larger zip code area) and updated data vintages for both the NLCD and the NCES.

The Analysis of variance (ANOVA) results for the predictive modeling are detailed in Table C-3. We applied this model to 75% of the LiDAR-derived tracts and assessed the predictive

accuracy using the remaining 25% of the LiDAR data. When comparing the predicted values to the actual values, we find that 68% of the estimates are within 10% of the actual values and 90% of the predicted values are within 20% of actual values. We note that these numbers are 8% to 10%greater (68% versus 60% and 90% versus 80%) than the original zip code assessment (Gagnon et al. 2016). The increase in predictability is likely a consequence of geospatially-resolved tract-level assessment, the increased number of tract observations, and the higher resolutions of the newer vintage data.

Table C-3. ANOVA of Small Building Suitability OLS Model

Source	DF	SS	MS	F	P-Value
Locale Description	3	0.29	0.10	8.87	0.0000
Census Division	8	23.93	2.99	272.41	0.0000
Developed—Open Space	1	5.38	5.38	489.62	0.0000
Developed—High Intensity	1	0.09	0.09	8.03	0.0046
Forest	1	0.67	0.67	60.96	0.0000
Water	1	0.07	0.07	6.50	0.0108
Northing	1	5.53	5.53	503.15	0.0000
Locale Description * Census Division	24	3.71	0.15	14.09	0.0000
Residuals	11,509	130.43	0.01	—	—

C.3. Rooftop Plane Area Model

The third model in the series is a predictive model used to predict the number and size of developable planes on a building. This predictive model follows a statistical distribution fitting approach. The number of developable surfaces is defined as the mean of a fitted exponential distribution for each building size class (i.e., small, medium, large). The number of suitable planes was calculated using a random sample from a national distribution of building suitable plane counts, per building size class (Table C-4).

Table C-4. National Distributions of Building Plane Count Probabilities by Building Size Class

Number of Planes	Small	Medium	Large
1	50%	21%	14%
2	28%	14%	7%
3	14%	13%	6%
4	5%	12%	5%
5	2%	10%	5%
6	1%	8%	5%
7	—	6%	5%
8	—	5%	4%
9	—	3%	4%
10	—	2%	4%
11	—	2%	3%
12	—	2%	3%
13	—	2%	3%
14	—	2%	3%
15–16	—	—	3%
17–20	—	—	2%
21–32	—	—	1%

Source: Gagnon et al. (2016).

Using a per building size class random sample, Gagnon et al. (2016) used the mean of the fitted probability density function to calculate the size of each developable plane. Because buildings with multiple planes were found to have a single plane larger than the remaining planes, the first plane in a building's sequence of multiple planes are fitted differently than the subsequent planes. Additionally, in in their assessments Gagnon et al. (2016) found that buildings with only one plane generally have a larger single plane. Therefore, to account for this, they built exponential fits for one-plane buildings separately from multi-plane buildings. These distribution fitting assessments were used here to inform the imputation of developable plane size. Table C-5 details the fitted areas assigned to each plane given the plane's sequential index and the building's size class. Confidence intervals for each plane's size were computed using the Gagnon et al. (2016) methodology for the 95th percentile range.

Table C-5. Fitted Areas for Each ith Plane, per Building Size Class

Building Size	iᵗʰ Plane	Fitted Area
Small	1	33.81 m²
	2–6	24.08 m²
Medium	1	800.00 m²
	2-14	31.74 m²
Large	1	4,000.00 m²
	2-32	181.81 m²

Source: Gagnon et al. (2016).

C.4. Rooftop Tilt and Azimuth Model

The rooftop tilt and azimuth model was developed by Gagnon et al. (2016) to predict the percent of rooftop planes with a particular tilt and azimuth class. This predictive model follows a statistical distribution fitting approach to predict the probability of plane having a particular tilt and azimuth given the buildings size and the number of planes on the building. For small buildings, per locale–type national average values are used from a lognormal fit of data in each of the azimuth-tilt classes. For medium and large buildings, we use national average values for each azimuth-tilt class. Table C-6 shows the national average tilt and azimuth distribution for building planes by building type used to sample a plane's orientation.

Table C-6. National Average Tilt/Azimuth Distribution for Building Planes, by Building Size Class

Building Size	Tilt	Azimuth					
		Flat	E	SE	S	SW	W
Small	0°	0.26					
	15°		0.03	0.02	0.06	0.02	0.03
	28°		0.09	0.06	0.18	0.06	0.09
	41°		0.02	0.02	0.03	0.01	0.02
	54°						
Medium	0°	0.74					
	15°		0.02	0.01	0.04	0.01	0.02
	28°		0.03	0.02	0.05	0.02	0.03
	41°				0.01		
	54°						
Large	0°	0.93					
	15°		0.01		0.01		0.01
	28°		0.01		0.01		0.01
	41°						
	54°						

Source: Gagnon et al. (2016).

Appendix D. Quantifying the Technical Potential and On-Site Consumption of LMI-Serving Buildings in Three Case Study Cities

We investigated the possible role for third-party buildings that serve low-income populations to host solar on their roofs. The specific building classes investigated are: Public sites (e.g., libraries, police stations, local government), Public housing (i.e., federally assisted rental housing), K–12 public schools, Homeless shelters, and Places of Worship. These building classes were chosen based on a combination of nonprofit status, a priori expectation of magnitude of potential, and feasibility in collecting GIS data. These building classes are not intended to be comprehensive of all third-party buildings that could deploy solar, and future analysis could examine potential for multiple other building classes, including on for-profit commercial buildings. Because of data limitations, estimates for these building classes are restricted to the cities of Chicago, Illinois; San Bernardino/Riverside, California; and Washington, D.C.

D.1. Quantifying the Technical Potential of Third-Party Buildings

To quantify the technical potential of LMI-serving buildings in the case study cities, we obtained GIS data for each building type and spatially tagged these layers to our LiDAR buildings data. This allowed us to identify the total technical potential for each building type in each city. Described in this appendix are the data sources and methods used to spatially join varied GIS layers of building locations to LiDAR building footprints.

The LMI-serving building data is an agglomerate data set sourced from a variety of locations, including both open and proprietary sources. Table D-1 lists all the data used to identify LMI-serving building footprints and then estimate the technical potential for each building class in our case study cities. Because the data consists of varied data sets and formats, we inevitably used varied methods to tag each building geometry to one or more LiDAR building footprints. Discussed below are the case-by-case methods used for each building type.

This report is available at no cost from the National Renewable Energy Laboratory (NREL) at www.nrel.gov/publications.

Table D-1. Core GIS Data Sources for LMI-serving Buildings in Case Study Cities

Building Type	City	Source
K–12 Public Schools	All	The National Center for Education Statistics' (NCES) *Core Common Data (CCD)*, 2015–2016.
Homeless Shelters	Chicago	Chicago's Department of Family and Support Services, *Homeless Services Map*. Downloaded from the Chicago Data Portal, 2017.
Homeless Shelters	Washington, D.C.	DC Department of Human Services', *Homeless Shelter Locations*. Downloaded from Open Data DC, 2017.
Homeless Shelters	San Bernardino; Riverside	Google Maps, 2017.
Places of Worship	All	Homeland Security Infrastructure Program (HSIP) Gold, 2013.
Public Housing	All	The National Housing Preservation Database (NHPD), 2016 *Active Properties*.
Public Sites	Washington, D.C.	2016 District Government Land (Owned, Operated, and or managed), from DC Government. Downloaded from Open Data DC.
Public Sites	Riverside	Riverside County, 2017.
Public Sites	Chicago	Libraries: Chicago Public Library Police Stations: City of Chicago Fire Stations: City of Chicago Senior Centers: City of Chicago; Family and Support Services Community Centers: City of Chicago; Family and Support Services Workforce Centers: City of Chicago; Family and Support Services County Government Administrative Facilities: Cook County Department of Facilities Management All data downloaded from the Chicago Data Portal, 2017 except for the county administration data, which was downloaded from Cook County Government Open Data, 2017.

53

K–12 Public Schools

Two data sets were used to geotag public schools with LiDAR building footprints: (1) the geocoded addresses from the National Center for Education Statistics' Common Core of Data (CCD), K12 Pubic data set (NCES CCD 2015-2016), and (2) campus boundaries from OpenStreetMap (OSM).[26]

Because each point in the CCD data set represents a single school's address location, we used the OSM school boundaries to help tag a single point to the set of buildings within the school campus. In the cases where an OSM boundary did not exist, we tagged the CCD school point to the nearest LiDAR building, using a maximum search radius of 500 meters. We ensured that no double-counting was occurring in the cases where multiple schools share the same building(s). Finally, technical potential was calculated from the aggregate of all school buildings, per city.

Homeless Shelters

Data for homeless shelters is an agglomerate data set. Where possible, we collected from individual city GIS repositories (i.e., Chicago and Washington, D.C.). For Chicago, we had to filter the Homeless Services data layer to include only homeless shelters. Where these authoritative government data sets did not exist (i.e., San Bernardino and Riverside), we collected coordinate data from Google Maps searches of homeless shelters in these cities. The resulting data set is an agglomeration point layer of homeless-shelter locations. We then tagged these homeless-shelter points to LiDAR buildings based on a nearest neighbor join, applying a maximum search radius of 500 meters. Finally, technical potential was calculated from the aggregate of homeless shelter buildings, per city.

Places of Worship

The places of worship layer was obtained from a single proprietary data source, the Homeland Security Infrastructure Program (HSIP) Gold (HSIP Gold 2013). Using this layer, we tagged the point locations to the LiDAR buildings polygons using a nearest neighbor method, applying a maximum search radius of 500 meters. We ensured that no buildings were being double-counted in the cases where more than one place of worship occupied the same building. Finally, technical potential was calculated from the aggregate of places of worship buildings, per city.

Public Housing

The public housing layer was obtained from a single data source, the 2016 Active Properties from the National Housing Preservation Database (NHPD 2016). Because the NHPD data set represents a single point location for multiple buildings that could span multiple parcels, we used the ownership attribution and parcel data to identify all the buildings belonging to a single NHPD property point. Parcel data was collected from individual government authorities (*see* Table D-2) and partial fuzzy join methods[27] were used to join parcel ownership attributes to NHPD property-owner attributes and identify all the parcels associated with each NHPD

---

[26] School boundaries were identified from a 2017 OSM United States extract, where "school" was tagged in the *building* and *amenity* keys.

[27] We set the partial fuzzy match cutoff to 80%. This was determined to be a conservative cutoff resulting in only a handful of false negatives and very few false positives.

property. We then tagged these parcels to the LiDAR building data to identify all buildings associated with a NHPD property. Care was taken to ensure that no two properties overlapped, and that double-counting was not occurring. The final technical potential was calculated from the aggregate of all public housing buildings, per city.

Table D-2. Parcel Data Used for Appropriating Buildings to Public Housing Properties

City	Source
Chicago	*Parcel 2015,* Cook County Clerk Map Department. Downloaded from Cook County Government Open Data.
Riverside	*Parcels* layer from the Assessor's County GIS geodatabase. Downloaded from Riverside County Open Data, 2017.
San Bernardino	County of San Bernardino's Geographic Information Services, *Parcel Basemap.* Retrieved from *FTP Services*, 2017.
Washington, D.C.	*Common Ownership Lots,* from the District's Vector Property Mapping Database. Downloaded from Open DC Data, 2017.

Importantly, Chicago's parcel data layer did not obtain ownership attribution. As a result, we were unable to tag NHPD points to all parcels associated with the property. Instead, we simply tagged the NHPD property points to the single intersecting parcel. Therefore, we are likely underestimating the total technical potential of public housing units in Chicago.

Public Sites

The public sites layer also is an agglomerate layer collected from a variety of sources. The layer consists of public site locations for Chicago, Riverside, and Washington, D.C. For both Washington D.C. and Riverside, we obtained the public sites data directly from the city or county data repositories. For Chicago, we collected the data in a piecemeal fashion from the city and county open data repositories. Filters were applied on these layers to include only sites pertaining to government administration buildings, rec centers, senior centers, community centers, workforce centers, libraries, police stations, and fire stations. For each public site, a LiDAR building were tagged based on a nearest neighbor algorithm, applying a maximum search radius of 500 meters. Care was taken to ensure no double counting of buildings in the cases where two public sites occupy the same building. Finally, technical potential was calculated based on the aggregate of the tagged buildings, per case study city.

We note two important qualifications regarding the public sites estimates. First, we were unable to identify public sites technical potential for San Bernardino, California, due to data limitations. Despite numerous requests, we were unable to obtain a public sites layer from the San Bernardino County. Second, this method assumes one building per site, and therefore, estimates of technical potential could be underestimated, especially for government administrative buildings which likely have multiple buildings per site.

D.2. Estimating the On-Site Consumption of Third-Party Buildings

To estimate the on-site consumption of LMI-serving third-party buildings in our case study cities, we used representative building loads from the 2009 Residential Energy Consumption Survey (RECS) or the 2012 Commercial Building Energy Consumption Survey (CBECS) (EIA

2013; EIA 2016a). Each building type was tagged to the most representative building in RECS or CBECS and was given the building consumption (kWh/year/ft^2) of that building type per Census Division. For each representative building, we calculated the average annual building consumption per roof area (kWh/year/ft^2), where roof areas were estimated from the number of floors and the total building area. Table D-3 describes the specific criteria used to tag each building type with its most appropriate building representative.

Table D-3. Representative Building Types Used for Third-Party Building Energy Consumption Estimates

Building Type	Energy Consumption Survey	Query Applied
K–12 Public Schools	CBECS 2012	Filter for education buildings identified as elementary, middle, or high schools.
Homeless Shelters	CBECS 2012	Filter for buildings with primary building activity of dormitory.
Places of Worship	CBECS 2012	Filter for religious worship buildings identified as places of worship.
Public Housing	RECS 2009	Filtered for buildings under the Public Housing Authority.
Public Sites	CBECS 2012	Filtered for state or local government-owned buildings where the primary building activity is one of the following. Administrative/professional office Government office Fire station/police station Other public order and safety Library Recreation Social/meeting Other public assembly Courthouse/probation office